#430

RADSAT

1 DEGREE LATITUDE-LONGITUDE

SORT, TRAPPED PARTICLES

72-076B-01A

Table of Contents

----

1. INTRODUCTION:

The documentation for this data set was originally on paper, kept in NSSDC's Data Set Catalogs (DSCs). The paper documentation in the Data Set Catalogs have been made into digital images, and then collected into a single PDF file for each Data Set Catalog. The inventory information in these DSCs is current as of July 1, 2004. This inventory information is now no longer maintained in the DSCs, but is now managed in the inventory part of the NSSDC information system. The information existing in the DSCs is now not needed for locating the data files, but we did not remove that inventory information.

The offline tape datasets have now been migrated from the original magnetic tape to Archival Information Packages (AIP’s).

A prior restoration may have been done on data sets, if a requestor of this data set has questions; they should send an inquiry to the request office to see if additional information exists.

2. ERRATA/CHANGE LOG:

NOTE: Changes are made in a text box, and will show up that way when displayed on screen with a PDF reader.

When printing, special settings may be required to make the text box appear on the printed output.

Version	Date	Person	Page	Description of Change
01				
02				

3 LINKS TO RELEVANT INFORMATION IN THE ONLINE NSSDC INFORMATION SYSTEM:

http://nssdc.gsfc.nasa.gov/nmc/

[NOTE: This link will take you to the main page of the NSSDC Master Catalog. There you will be able to perform searches to find additional information]

4. CATALOG MATERIALS:

a. Associated Documents — To find associated documents you will need to know the document ID number and then click here. http://nssdcftp.gsfc.nasa.gov/miscellaneous/documents/

b. Core Catalog Materials

RADSAT

1 DEG. LAT-LONG SORT OF TRAPPED PARTICLES

72-076B-01A SPMS-00133

THIS DATA SET HAS BEEN RESTORED. IT ORIGINALLY CONTAINED ONE 9-TRACK, 1600 BPI TAPE WRITTEN IN BINARY. THERE IS ONE RESTORED TAPE. THE DR TAPE IS A 3480 CARTRIDGE AND THE DS TAPE IS 9-TRACK, 6250 BPI. THE ORIGINAL TAPE WAS CREATED ON A CDC 6600 COMPUTER AND WAS RESTORED ON AN IBM 9021 COMPUTER. THE TIME SPAN IS NOT IN THE FORMAT OR ON THE TAPE ITSELF. THE DR AND DS NUMBER ALONG WITH THE CORRESPONDING D NUMBER AND TIME SPAN IS AS FOLLOWS:

DR#	DS#	D#	FILES	TIME SPAN
DR005879	DS005879	D031991	5	10/02/72 - 02/28/73

REQ. AGENT	RAND NO.	ACQ. AGENT
CMP	RD0812	DMS

RADSAT

1 DEG. LAT-LONG SORT OF TRAPPED PARTICLES

72-076B-01A

This data set contains 1 data tape. It is a 9 track, binary, 1600 BPI tape with 5 files. It was created on a CDC computer. The time span is not in the format or on the tape itself.

D#	C#	TIME COVERAGE
D-31991	C-20126	10/02/72 - 02/28/73

Reprint from:

72-076B-01A
DSC #430

COSPAR

SPACE RESEARCH XIV

Proceedings of Open Meetings of Working Groups of the Sixteenth Plenary Meeting of COSPAR

Constance, F.R.G. — 23 May—5 June 1973

and

Resumés of the
Symposium on Noctilucent Clouds and Interplanetary Dust

Constance, F.R.G. — 24 and 25 May 1973

Edited by

M. J. RYCROFT
R. D. REASENBERG

AKADEMIE-VERLAG · BERLIN

1974

Space Research XIV — Akademie-Verlag, Berlin 1974

OBSERVATIONS OF 5–45 MeV PROTONS AT $L \lesssim 3$ AND $L \gtrsim 7$

R. C. Filza[a], L. Katz[a], P. L. Rothwell[a], B. Sellers[b], F. A. Hanser[b] and E. Holeman[c]

[a]Air Force Cambridge Research Laboratories, Bedford, Mass., USA
[b]Panametrics, Inc., Waltham, Mass., USA
[c]Franklin Pierce College, Rindge, New Hampshire, USA

This paper reports new results on trapped proton and solar proton fluxes obtained in late 1972. The data were obtained aboard satellite 1972-076B launched on 2 October 1972 by an instrument which detects protons from 5 to 45 MeV in five energy channels. The high inclination of the satellite orbit permits the study of both magnetospherically trapped proton fluxes in the South Atlantic anomaly and solar proton fluxes over the polar regions. The L-dependence and pitch-angle dependence of trapped protons with $H_{\min}$ between 700 and 760 km are presented and the data are compared with earlier data taken at low altitude. The time-dependence, energy spectra and pitch-angle distribution of solar protons measured during the solar event of 30 October–2 November 1972 are also presented and discussed.

1. Introduction

The particle instrument flown on Air Force satellite 1972 076-B, apogee 750 km, perigee 729 km, inclination 98.4°, performs a simultaneous six-channel energy analysis and identification of protons, deuterons, tritons, helium three and alpha particles. The detector contains four solid state detectors arranged as a telescope and a photomultiplier-plastic scintillator anticoincidence shield. The telescope has a 6° half angle view cone and a geometric factor of 0.0257 cm^2 sr. The total energy analysis is performed by two 300 mm^2, 5 mm thick lithium drifted silicon detectors acting as a single 10 mm detector. The plastic scintillator anticoincidence shield strongly reduces false counts from side or rear entering particles. The signals from the various components of the telescope are combined to obtain, a particle identifier signal in five bins and a total energy signal in six bins yielding a matrix of 30 channels which are accumulated and telemetered. For protons the energy channels are 5.0–7.0 MeV, 7.0–12.2 MeV, 12.2–18.2 MeV, 18.2–28 MeV and 28–45 MeV, with an additional channel to indicate protons of an energy not normally capable of depositing sufficient energy to trigger the counter without causing an anticoincidence.

All aspects of the system appear to be operating normally as evidenced, for example, by the operation of the detectors while spinning through the trapped proton mirror plane in the South Atlantic. The lack of noise in the data as received is exemplified in the 28–45 MeV trapped proton pitch angle distribution shown in Fig. 1.

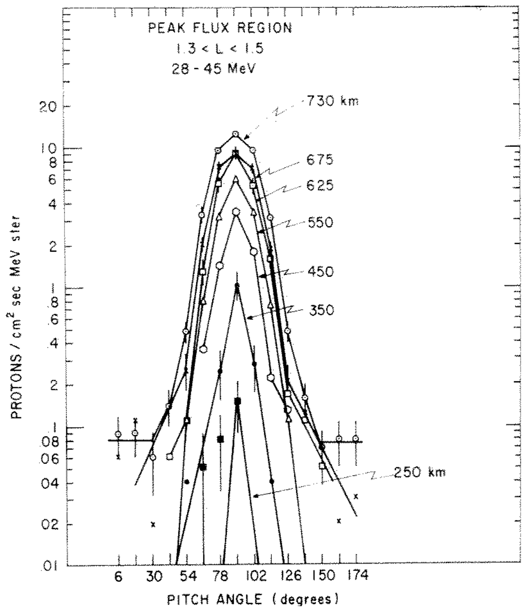

Fig. 1. The 28—45 MeV proton pitch angle distribution measured for H_{min} 250—730 km and $1.3 \leqq L \leqq 1.5$.

2. Trapped Proton Observations

In order to analyze the large amount of data received, it was first necessary to divide the measurements into intervals of McIlwain's L parameter [1] and B, the magnetic field strength. In this case H_{min}, the minimum altitude reached by the trapped proton guiding center in its longitudinal drift, was used in place of B. B was determined to be a linear function of H_{min} for constant L. Fig. 1 shows the pitch angle distribution of 28—45 MeV protons measured in the peak flux region for different intervals of H_{min}. The distributions are narrower at lower H_{min} due to losses below ~200 km.

Since the background is negligible, we have obtained omnidirectional trapped proton fluxes from the data by simply dividing the total counts into 0.1 earth radii intervals of L and 10 km intervals of H_{min}. For the period 7 October to 6 November 1972, the L distribution of the omnidirectional proton fluxes is shown in Fig. 2 for H_{min} between 700 and 760 km. Wide differences are exhibited here in the location of maximum flux from the lowest energy of 6 MeV with a peak between L 2.0 and 2.4, and from 28—45 MeV with a sharp peak at $L = 1.4$.

Utilizing the 700—765 km H_{min} data for the 7 October—6 November 1972 period, we have also derived energy spectra which exhibit three general shapes: (i) at low L values 1.1—1.4 very flat; (ii) at middle L values 1.4—2.2 fairly steep with fairly characteristic breaks at 9 and 15 MeV; (iii) at high L values greater than 2.2 very steep spectra with slope increasing with L. These spectra are very similar to observations made earlier by other experimenters [2]. The altitude dependence of the omnidirectional peak fluxes for appropriate L intervals is smoothly varying with altitude; however, they cannot be fit by a single power law with altitude.

In order to compare our 1972 measurement with nuclear emulsion measurements made with recoverable satellites in 1961—1962, we constructed a model to fit the 1972 data. The model was extrapolated to 55 MeV at each individual

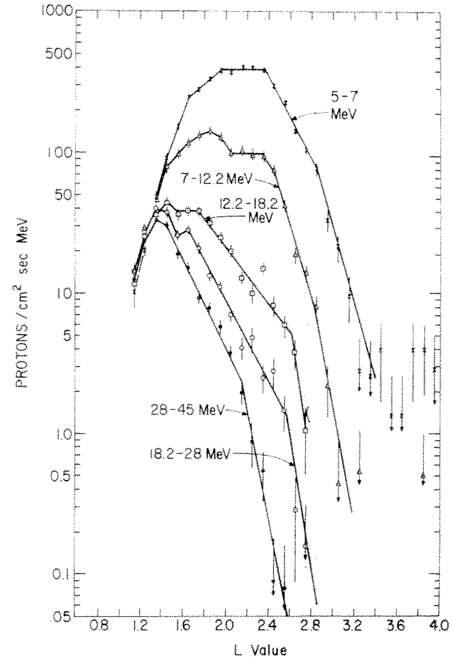

multiply by π/2 for correction!

Fig. 2. The L dependence of the trapped proton fluxes for the five energy bins for the period 7 October—6 November 1972 and the H_{min} interval 700—765 km. The errors are purely statistical and the solid lines are drawn to indicate the data trend.

H_{min}, L point and integrated over the satellite orbits used in the nuclear emulsion 1961—1962 study by Filz et al. [3]. A correlation of the 1961—1962 55 MeV flux data shows excellent agreement which indicates that over the 11-year solar cycle the fluxes have returned to their original value. The 1972 data are also compared with data obtained by Achtermann et al. [4] for two different L shells. The fluxes recorded by Achtermann et al. appear a factor of $\sim$2 higher at 20 to 50 MeV and as much as a factor of $\sim$10 higher at the lower energies. While the 20—50 MeV difference can be expected from solar cycle changes, it is not clear that such a drastic change in the 6 MeV protons is due to this cause.

3. Solar Particles

Solar protons were observed at high latitudes during the 29 October—1 November 1972 time period. In this paper we would like to concentrate on the fluxes, energy spectra and pitch-angle distributions of these particles. The 5—7 MeV channel first detected solar protons on 29 October 1972 at ~2300 h UT. The flux recorded in this channel peaked at ~1200 h UT on 31 October at 70 protons/(cm²-MeV-sec). By 0300 h UT on 1 November the flux had decreased to 3 protons/(cm²-MeV-sec). The 28.0—45.0 MeV proton channel, on the other hand, recorded a flux maximum of 0.08 protons/(cm²-MeV-sec) at ~0100 h UT on 31 October, or approximately 11 hours before the 5—7 MeV proton flux

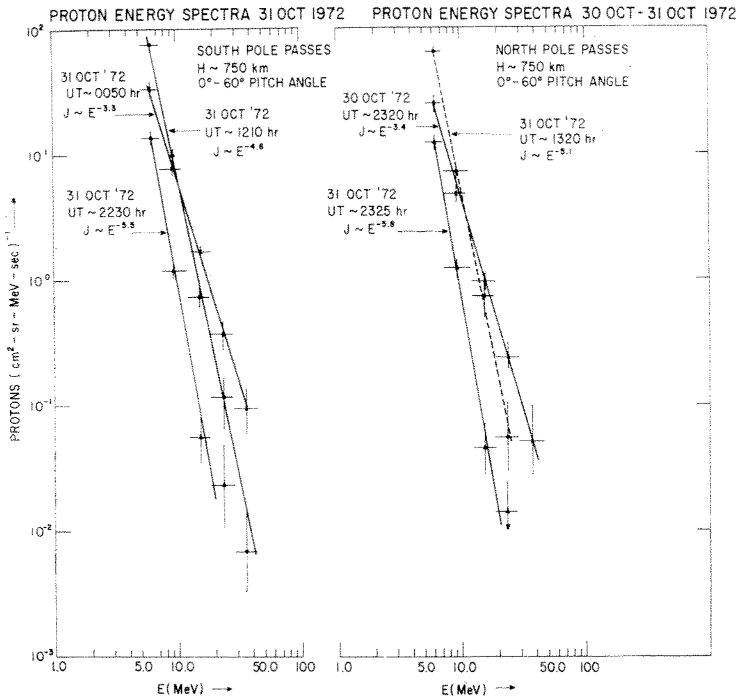

Fig. 3. Solar proton energy spectra measured over the North and South poles at similar times.

peaked. The time-histories show excellent agreement with those measured outside the magnetosphere by satellite OV 5—6 [5]. The South Pole passes showed a slightly higher flux than the North Pole passes, an asymmetry pointed out by Evans and Stone [6]. The three other proton channels whose energy limits are between those of the other two channels show similar behavior.

Proton energy spectra are shown in Fig. 3. A single power law function fits the proton spectra over the energy region of interest. These spectra are similar to those reported for the large 28 May 1967 solar event by Lanzerotti [7]. North and South polar passes taken within less than one hour of one another show no significant difference in spectral shape. Over larger periods of time spectra become characteristically softer.

Fig. 4 shows some pitch-angle distributions of 5—7 MeV solar protons. The flux decreases rapidly beyond 90° due to the atmospheric loss cone. The data were separated into north-south, day-night passes. The symbol $\bar{\Lambda}$ denotes the average invariant latitude over which the distribution was taken. The two curves for each pass correspond to data taken on the polar plateau and between the high-latitude cutoff and the flux peaks. The data indicate that the solar particle flux is isotropic in the upper hemisphere, except perhaps over the North Pole at local night. The seemingly higher fluxes along the field line for this particular pass could, however, be due to statistical fluctuations.

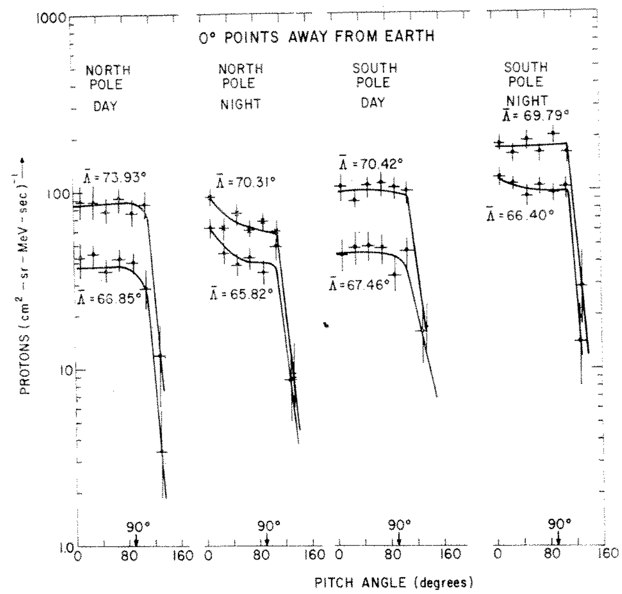

Fig. 4. Pitch-angle distributions of 5—7 MeV solar protons for north and south, day and night passes 31 October 1972. The vertical error bars denote the statistical uncertainty in the flux and the horizontal error bars the 20° angular interval over which the data were taken.

4. Conclusions

A preliminary analysis of proton data obtained from the particle instrument on Air Force satellite 72-1 has yielded important information on trapped protons in the South Atlantic at this phase of the solar cycle. When extrapolated to 55 MeV energy and integrated over the same orbits, the 1972 data are in agreement with nuclear emulsion data taken in 1961—1962 at the same phase of the solar cycle. Solar protons during the 29 October—1 November period were also measured on the S72-1 satellite. The 28.0—45.0 MeV proton flux reached its maximum value approximately 11 hours before the 5—7 MeV proton flux. The proton energy spectra progressively softened with time and were consistent with a single power law fit. The 5—7 MeV proton flux was isotropic in the upper hemisphere.

References

[1] C. E. McILWAIN, J. Geophys. Res. **66**, 3681 (1961).
[2] See e.g. W. H. HESS, The Radiation Belt and Magnetosphere, Blaisdell Publ. Co., Waltham, Mass. 1968.
[3] R. C. FILZ and E. HOLEMAN, J. Geophys. Res. **70**, 5807 (1965).
[4] E. ACHTERMANN, S. C. FREDEN and D. HOVESTADT, Report, Max-Planck-Institut für Physik und Astrophysik, Extraterr. 6/67 (May 1967).
[5] L. KATZ, P. L. ROTHWELL, G. K. YATES, B. SELLERS and F. A. HANSER, Proc. 7th ESLAB Symp. on Correlated Interplanetary and Magnetospheric Observations, D. Reidel Publ. Co., Dordrecht, Holland 1974 (p. 413).
[6] L. C. EVANS and E. C. STONE, J. Geophys. Res. **74**, 5127 (1969).
[7] L. J. LANZEROTTI, J. Geophys. Res. **74**, 2851 (1969).

Note added in proof. The omnidirectional trapped proton fluxes presented in Fig. 2 should be multiplied by $\pi/2 = 1.57$. This allows slightly better agreement with the Achtermann data (see text) but has little effect on the correlation with the emulsion results of Filz and Holeman [3]. This is a correction related to the spinning of the detector through the trapped mirror plane distribution and does not change either the directional fluxes or the solar particle fluxes.

VOL. 82, NO. 13 JOURNAL OF GEOPHYSICAL RESEARCH MAY 1, 1977

72-076B-01A
DSC #430

Geomagnetically Trapped Alpha Particles From 18 to 70 MeV

A. G. RUBIN, R. C. FILZ, AND P. L. ROTHWELL

Air Force Geophysics Laboratory, Hanscom Air Force Base, Massachusetts 01731

B. SELLERS

Panametrics, Inc., Waltham, Massachusetts 02154

The energy spectrum of alpha particles trapped in the magnetosphere has been measured for the first time between 18 and 70 MeV for L values from 1.85 to 2.85 at 740-km altitude. In this energy range the spectrum is described by a power law with exponent 5.5 ± 1.3. The L distributions of alphas and protons with the same energy per nucleon are similar, but at the same energy per particle, distributions are distinctly different. The alpha to proton ratio maximum is 3.5×10^{-3}, an order of magnitude lower than that in the solar wind, and it falls steeply with energy.

INTRODUCTION

The average properties of radiation belt protons and electrons are now fairly well known. The origin of the inner trapped proton belt has been fairly well explained by the neutron albedo theory combined with inward radial diffusion [*Claflin and White,* 1974]. The origin, distribution, and loss mechanisms of the remaining trapped ions are less well understood. It is not known to what extent trapped ions are directly captured from the solar wind and, if they are, whether by direct penetration through the magnetospheric boundary, diffusion through the flanks of the magnetosphere, or direct injection in the polar regions.

In the direct capture mechanism the low-energy particles of the solar wind can interact strongly with the magnetic fields at the magnetospheric tail boundary where the ratio of particle energy density to magnetic field energy density is unity and none of the adiabatic invariants are conserved. In these turbulent boundary regions, low-energy particles can penetrate into the magnetic field. If these low-energy particles subsequently diffuse inward under the action of turbulent electric and magnetic field conserving the first two adiabatic invariants, they will gain energy. This diffusion-energizing process has been described by *Walt* [1971], *Schulz and Lanzerotti* [1974], and *Cornwall* [1971, 1972].

Bird [1975] has discussed capture of solar wind particles and their subsequent trapping. *Van Allen and Randall* [1971] have given evidence of direct capture of energetic alpha particles into trapping regions, and *Lanzerotti* [1968] has presented an example of energetic alpha particle direct penetration into high L regions.

In addition to the above mechanisms, it is also possible for alpha particles to originate in the polar wind and subsequently to be energized [*Axford,* 1970].

In the present work the trapped alpha particle population has been measured between 18 and 70 MeV for the region between $B = 0.22$ G, $L = 1.85$ and $B = 0.25$ G, $L = 2.85$.

The study of the properties of trapped alpha particles can serve to distinguish between various mechanisms which lead to trapped particles. The most abundant heavy charged particle species after protons is alpha particles, whose existence in the radiation belts was first confirmed by *Krimigis and Van Allen* [1967]. Additional information on alpha particle populations was obtained by *Fritz and Krimigis* [1969], *Krimigis* [1970, 1973], *Blake and Paulikas* [1970, 1972], *Blake et al.* [1973], *Fennell et al.* [1974], *Krimigis and Verzariu* [1973], and *Fritz and Williams* [1973].

Recently, observations at synchronous altitudes have disclosed very substantial populations of alpha particles in the ring current, perhaps exceeding the proton population (S. DeForest, private communication, 1976). In fact, *Tinsley* [1976] and *Lyons and Evans* [1976] have proposed that the ring current late in a recovery phase is largely composed of He^+. This proposal is supported by measurements of low-altitude ions [*Mizera and Blake,* 1973; *Blake,* 1976]. If, indeed, the ring current is made up of particles transported to synchronous altitudes by the polar wind (S. DeForest, private communication, 1976), there is then an ample source of magnetospheric helium at ring current altitudes.

The population of alpha particles in the inner zone would then depend on the diffusion of ring current helium inward, competing with loss of helium by charge exchange.

INSTRUMENTATION

These measurements of trapped alpha particles were made by a particle identifier instrument on board the S72-1 (1972-076B) satellite. The satellite was launched October 2, 1972, into a polar orbit with an inclination of 98.4°, an apogee of 749 km, and a perigee of 731 km. It spins, with axis normal to the orbit plane, at approximately 12 rpm. The reported data were accumulated while the satellite spun through the trapped particle mirror plane in the South Atlantic anomaly. Since the instrument is mounted with its acceptance cone perpendicular to the satellite spin axis, it completed a 180° pitch angle scan in 2.5 s. Previously reported measurements made by use of this particle identifier include those of 5- to 45-MeV trapped and solar flare protons [*Filz et al.,* 1974], solar flare deuterons and tritons [*Rothwell et al.,* 1973], and alpha to proton ratios [*Katz et al.,* 1974]. Design and calibration details have been given by *Sellers et al.* [1973].

The detector assembly for the instrument shown in Figure 1 contains four solid state detectors arranged as a telescope and photomultiplier–plastic scintillator anticoincidence shield.

The geometrical solid angle is defined by two 100 mm², ~100-μm-thick totally depleted detectors arranged with tungsten collimators in front to minimize edge effects. The energy deposited in the first of these, the ΔE detector, is called E_d, and that deposited in the second, or geometry-defining, detector is called E_g. The telescope has a 6° average half angle view cone

Paper number 7A0058.

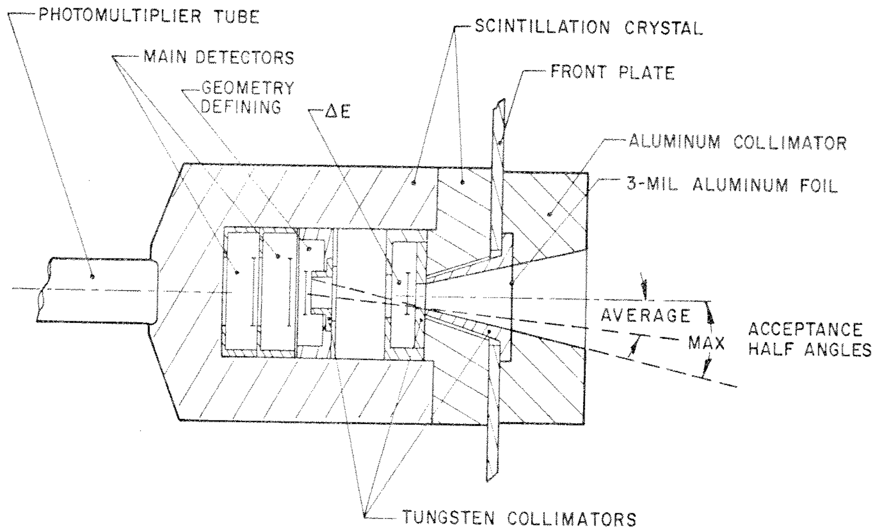

Fig. 1. Detector assembly geometry of S72-1 particle identifier.

and a geometric factor of 0.0257 cm² sr. The bulk of the total energy analysis is performed by two 300 mm², 5-mm-thick lithium-drifted silicon detectors connected electrically in parallel to act as a single 10-mm-thick detector. This is called the main detector, and the energy deposited in it is called E_m. The plastic scintillator anticoincidence shield strongly reduces false counts from particles not entering the aperture and from those energetic particles which enter the aperture and pass through the main detector.

The particle identification principle is similar to that used in the Explorer 34 and 41 satellites [*Lanzerotti et al.*, 1969]. The principal instrumental differences are the inclusion of the anticoincidence shield and the use of a main detector 10 mm in thickness. The shield is essential for measurement of trapped radiation, particularly energetic alpha particles, and the thicker detector allows the use of the identification method up to 45 meV for protons. This method relies on the fact that for a particle of incident energy E the stopping power $S(E)$ is given by

$$S(E) = dE/dx = F(M, z^2)f(E)/E \qquad (1)$$

where $F(M, z^2)$ is a function of the mass M and charge z of the particle and $f(E)$ is slowly varying (logarithmic) function of E. Hence $ES(E)$ is a quantity that varies little with energy and is characteristic of the particle. The particle identification signal P used here approximates that characteristic quantity as follows:

$$P = E_d(E_0 + K_dE_d + K_gE_g + E_m) \qquad (2)$$

where E_0, K_d, and K_g are constants chosen by analysis to minimize the variation of P over the energy region of interest.

Figure 2 shows a comparison of theoretical calculations with experimental calibrations carried out at the Yale University heavy ion linear accelerator. For the flight unit, $K_g = 1.03$. The energy E is determined from the measured total deposited energy E_t,

$$E_t = E_d + E_g + E_m \qquad (3)$$

and the calculated energy loss in the aluminum foil.

Also shown in Figure 2 are typical results for the experimentally measured full width at half maximum of the quasi-Gaussian P distribution. Factors that contribute to this width include detector and other electronic noise, energy straggling in the detectors, and, during accelerator calibration, the distribu-

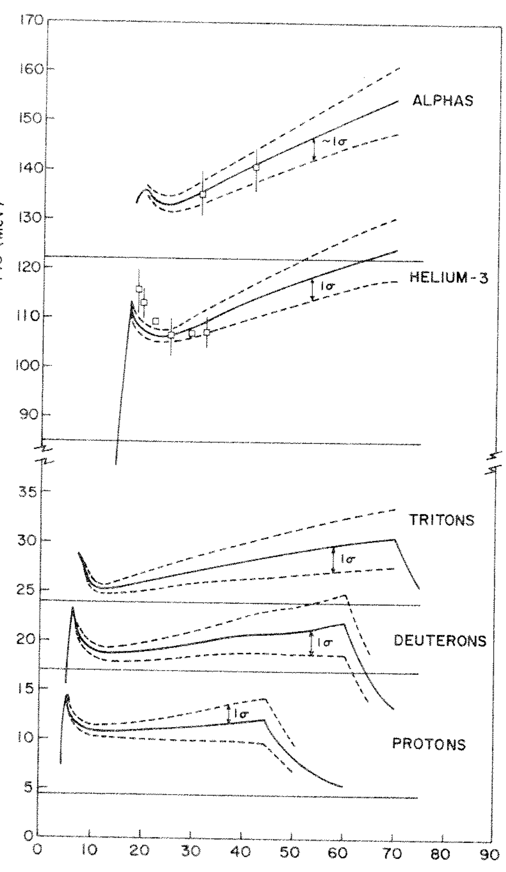

Fig. 2. Comparison of experimental and theoretical particle identification signal results.

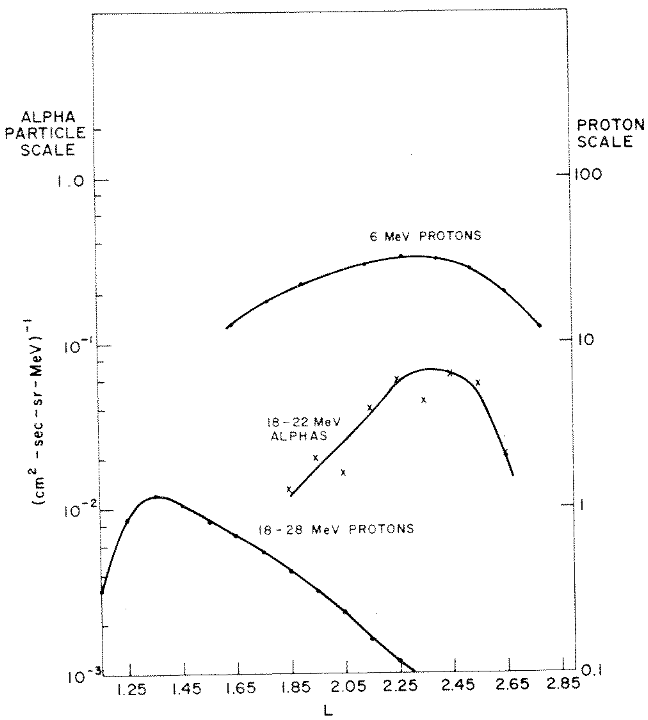

Fig. 3. The L distribution of protons and alpha particles measured on S72-1 at an altitude of 740 km for the period from October 1972 through February 1973.

tion of the beam about its average energy E. By taking all but the last of these various factors into account in a computer model, one obtains the theoretical cross contamination of one particle channel by another [*Sellers et al.*, 1973, Table 4.2]. The theoretical 1-standard-deviation limits, denoted by the dotted curves in Figure 2, were found to be consistent with the accelerator data. The separation of the alpha particle channel from the proton channel is sufficiently large that there is essentially no possibility of contamination of either by the other. In fact, measurements in the inner zone show that contamination of the alpha particle channel by protons is less than 5×10^{-4} at the same total energy. This ratio will of course be much less in terms of MeV per nucleon for the steep energy spectra considered here. Because the ^{3}He flux is quite small in comparison with the alpha particle flux and, in addition, the ^{4}He signal is separated by 3.5 standard deviations from the ^{3}He signal, the contamination by ^{3}He nuclei of the ^{4}He channels is also negligible. The ^{4}He channel had an upper level discriminator at 170 $(MeV)^2$ and is not sensitive to heavier ions.

In the flight instrument a built-in electronic circuit combines the E_d, E_g, and E_m signals to sort the P signals into five windows and the corresponding E_t signals into six windows, thus yielding a matrix of 30 channels [*Sellers et al.*, 1973, Table 2.2]. All channels are read out simultaneously once each 0.08 s, which corresponds to only 5.7° at the 12-rpm satellite spin rate. In combination with the narrow 6° acceptance cone half angle this allows pitch angle resolution of the order of 12°.

EXPERIMENTAL RESULTS

The Energy Spectrum

The energy spectrum of trapped alpha particles has not previously been measured for energies greater than 10 MeV. The energy range measured here is from 20 to 70 MeV in four energy windows, 18-22.5, 22.5-31.7, 31.7-47.2, and 47.2-70 MeV. The paucity of data necessitates averaging the alpha particle spectra over the L region between 1.85 and 2.65. Figure 3 shows that the alpha flux in the 18-22 MeV range peaks in the region from L = 2.15 to 2.55 and falls off steeply, declining by a factor of 2 at L = 2.15 and 2.60. The peak at L = 2.35 and sharp falloff are consistent with the finding by *Blake et al.* [1973] which indicates that the flux of 7-MeV alpha particles varies by an order of magnitude between L= 1.85 and L = 2.1.

The energy spectrum of alphas, shown in Figure 4, is obtained by averaging over the range of L, B, and the time indicated above.

The spectrum may be described by a power law within the statistical error with the flux, falling approximately as the fifth power of the energy. The power law exponent 5.5 ± 1.3 is consistent with the data within experimental error.

The alpha spectra may be compared with the measurements of *Fennell et al.* [1974]. Their spectra are described by a power law with exponents varying between 2.4 at L = 2.3-2.4 and 4.9 at L = 3.3-3.4 for alpha energies up to 10 MeV. The spectrum measured here over an L range from 1.85 to 2.65 is somewhat steeper. *Blake et al.* [1973] find a flat alpha particle spectrum for energies below about 7 MeV, for $1.85 < L < 2.15$. The present measurements did not extend to this energy. *Fennell et al.* [1974] show spectra which are power law at high energies but which flatten out at lower energy.

Pitch Angle Distributions

Figure 5 shows the pitch angle distribution of the alphas compared with the proton pitch angle distribution. These are the same within statistics and indicate that both pitch angle distributions are determined by atmospheric losses which cut off the distributions sharply for angles less than 90°.

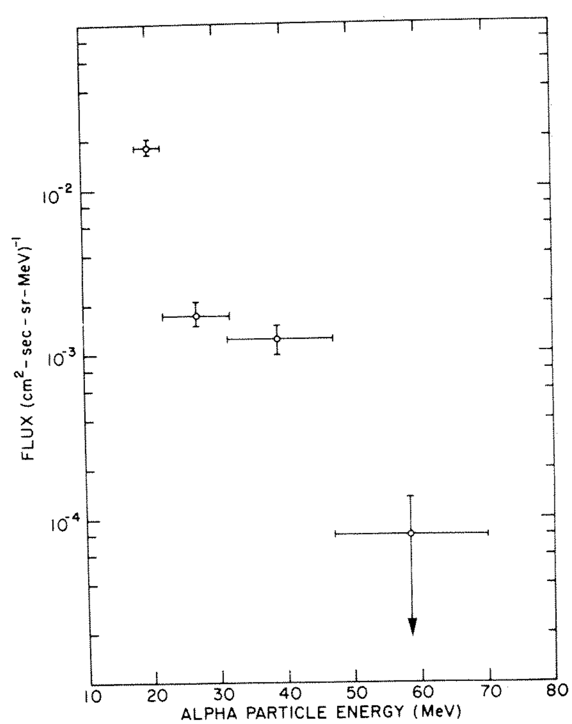

Fig. 4. The energy spectrum of alpha particles measured on S72-1. Data shown in this figure, Figure 5, and Figure 6 are integrated over the range $1.85 \leq L \leq 2.65$ at an altitude of 740 km for the period from October 1972 through February 1973.

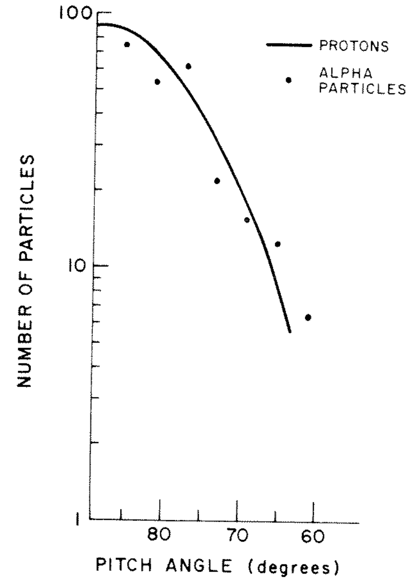

Fig. 5. Pitch angle distributions of alpha particles and protons.

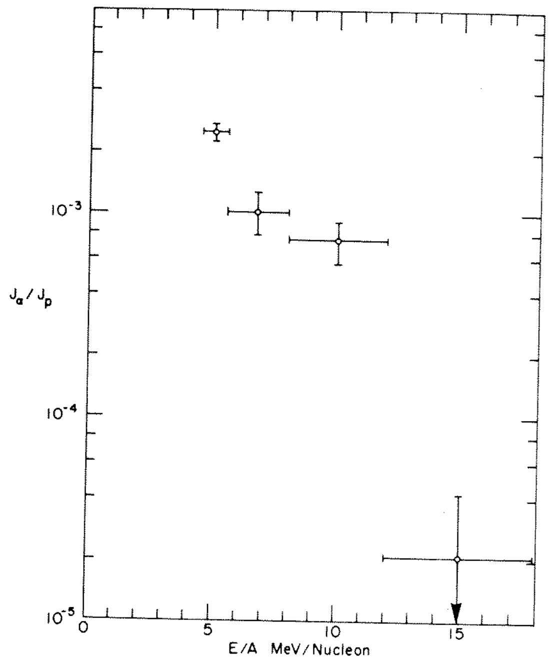

Fig. 6. The alpha to proton ratio versus energy per nucleon as measured on S72-1.

Radial Distribution of Alphas

Comparison of the L distribution of 20-MeV alphas with that of protons of the same energy and also with that of protons of the same energy per nucleon shows significant differences (Figure 3). It is clear that the L distribution is similar for protons and alphas of the same energy per nucleon and quite different for protons and alphas of the same energy. The proton and alpha distributions both fall off rapidly at $L = 2.6$; the inner boundaries of the proton and alpha particle distributions are, however, considerably different. The 25-MeV proton distribution peaks at $L = 1.35$, while the 20-MeV alpha particle distribution peaks at $L = 2.40$. The inner boundary of the trapped proton distribution has been calculated in detail and is well accounted for by losses due to charge exchange and coulomb collisions by bound and free electrons. In the proton case the source of particles is a combination of albedo neutron decay and diffusion from higher L. *Blake et al.* [1973] have provided evidence that a large proportion of the trapped alpha particles is due to diffusion inward from larger L, although the direct injection mechanism [*Van Allen and Randall*, 1971; *Lanzerotti*, 1968] may be effective at higher energies.

The L distribution of alpha particles obtained here provides an opportunity for another test of the charged particle injection and loss mechanism studied for the proton population. There are sufficient ambiguities and uncertainties in the theory [*Chaflin and White*, 1974] that a test with another species is highly desirable. The similarity between the radial distributions of alphas and protons at the same energy per nucleon rather than at the same total energy has previously been noted, but so far there has been no explanation. *Tverskoy* [1965] predicted that the L value of the peak of the alpha particle distribution at a given energy would be at the same position as the peak of the proton distribution for protons of one fourth the energy, thermalization at the magnetopause being assumed. This calculation made use of magnetic fluctuation driven diffusion and coulomb losses. *Cornwall* [1972], employing an electrostatic diffusion mechanism and charge exchange as well as coulomb losses, predicted a small displacement between proton and alpha peaks for similar energy per nucleon.

Alpha to Proton Ratio

Figure 6 shows the alpha to proton ratio plotted versus energy per nucleon obtained in the present work. In the energy range covered here, higher than has previously been measured, the α/p ratio falls off steeply with energy. The maximum value of 2.5×10^{-3} at 4.5 MeV/nucleon is close to the value of 3.5×10^{-3} reported by Fennell et al. at $L = 2.6$–2.7 from measurements made on OV1-19 in 1969 at a higher altitude at energies up to 1.8 MeV/nucleon.

From Figure 3 it can be seen that the alpha to proton ratio is peaked at $L = 2.5$. This was also found to be true at lower energy by *Fennell et al.* [1974]. If one extrapolates the α/p ratio of Fennell, Blake, and Paulikas to the higher energy per nucleon range of the present work, the α/p ratio measured here is higher by about a factor of 10. This discrepancy can perhaps be understood by the following considerations. *Krimigis* [1970] has found that the α/p ratio rises dramatically following a magnetic storm and subsequently decays. In the present measurements, averaged over a 4-month period, the enhanced α/p ratios typical of storm times are most likely predominant. During the time period of the measurements a magnetic storm occurred on October 31–November 1, 1972. The α/p ratio may be higher than is typical of quiescent periods.

Our measurements of alpha to proton flux ratios are in the vicinity of 10^{-3}. According to Cornwall, values of alphas to protons less than 10^{-4} indicate a fully thermalized particle source, so that values in the range of 10^{-4} indicate incomplete thermalization. If the alphas entered the magnetosphere through the bow shock, they would be fully thermalized by the shock transition. Subsequently, direct entry into the magnetosphere is possible through the cusps or through the flanks, both of which would most likely preserve thermalization.

Acknowledgment. The Editor thanks T. A. Fritz for his assistance in evaluating this report.

REFERENCES

Axford, W. L., On the origin of radiation belt and auroral primary ions, in *Particles and Fields in the Magnetosphere,* edited by B. M. McCormac, p. 46, D Reidel, Dordrecht, Netherlands, 1970.

Bird, M. K., Solar wind access to the plasma sheet along the flanks of magnetotail, *Planet. Space Sci., 23,* 27, 1975.

Blake, J. B., On the ionic identity of the ring current particles, *J. Geophys. Res., 81,* 6189, 1976.

Blake, J. B., and G. A. Paulikas, Measurements of trapped alpha particles $2 \leq L \leq 4.5$, in *Particles and Fields in the Magnetosphere,* edited by B. M. McCormac, D. Reidel, Dordrecht, Netherlands, 1970.

Blake, J. B., and G. A. Paulikas, Geomagnetically trapped alpha particles, 1, Off-equator particles in the outer zone, *J. Geophys. Res., 77,* 3431, 1972.

Blake, J. B., J. F. Fennell, M. Schulz, and G. A. Paulikas, Geomagnetically trapped alpha particles, 2, The inner zone, *J. Geophys. Res., 78,* 5498, 1973.

Claflin, E. S., and R. S. White, A study of equatorial inner belt protons from 2 to 200 MeV, *J. Geophys. Res., 79,* 959, 1974.

Cornwall, J. M., Transport and loss processes for magnetospheric helium, *J. Geophys. Res., 76,* 264, 1971.

Cornwall, J. M., Radial diffusion of ionized helium and protons: A probe for magnetospheric dynamics, *J. Geophys. Res., 77,* 1956, 1972.

Fennell, J. F., J. B. Blake, and G. A. Paulikas, Geomagnetically trapped alpha particles, 3, Low-altitude outer zone alpha-proton comparisons, *J. Geophys. Res., 79,* 521, 1974.

Filz, R. C., L. Katz, P. L. Rothwell, B. Sellers, F. A. Hanser, and E. Holeman, Observations of 5–45 MeV protons at $L \lesssim 3$ and $L \gtrsim 7$, *Space Res., 14,* 321, 1974.

Fritz, J. A., and S. M. Krimigis, Initial observations of geomagnetically trapped protons and alpha particles with Ogo 4, *J. Geophys. Res., 74,* 5132, 1969.

Fritz, J. A., and D. J. Williams, Initial observations of geomagnetically trapped alpha particles at the equator, *J. Geophys. Res., 78,* 4719, 1973.

Katz, L., P. L. Rothwell, G. K. Yates, B. Sellers, and F. A. Hanser, Simultaneous observation of proton and alpha fluxes during the period 29 October–3 November 1972, in *Correlated Interplanetary and Magnetospheric Observations,* edited by D. E. Page, D. Reidel, Dordrecht, Netherlands, 1974.

Krimigis, S. M., Alpha particles trapped in the earth's magnetic field, in *Particles and Fields in the Magnetosphere,* edited by B. M. McCormac, p. 364, D. Reidel, Dordrecht, Netherlands, 1970.

Krimigis, S. M., The charge composition aspect of energetic trapped particles, paper presented at Solar Terrestrial Relations Conference, Nat. Res. Counc./Univ. of Calgary, Calgary, Alberta, Canada, 1973.

Krimigis, S. M., and J. A. Van Allen, Geomagnetically trapped alpha particles, *J. Geophys. Res., 72,* 5779, 1967.

Krimigis, S. M., and P. Verzariu, Measurements of geomagnetically trapped alpha-particles, 1968–1970, 1, Quiet times distributions, *J. Geophys. Res., 78,* 7275, 1973.

Lanzerotti, L. J., Penetration of solar protons and alphas to the geomagnetic equator, *Phys. Rev. Lett., 21,* 929, 1968.

Lanzerotti, L. J., H. P. Lie, and G. L. Miller, A satellite solar cosmic ray spectrometer with on-board particle identification, *IEEE Trans. Nuc. Sci., 16*(1), 343, 1969.

Lyons, L. R., and D. S. Evans, The inconsistency between proton charge exchange and the observed ring current decay, *J. Geophys. Res., 81,* 6197, 1976.

Mizera, P. F., and J. B. Blake, Observations of ring current protons at low altitudes, *J. Geophys. Res., 78,* 1058, 1973.

Rothwell, P. L., L. Katz, B. Sellers, and F. A. Hanser, Upper limits to flare-produced deuterium and tritium, *Phys. Rev. Lett., 31,* 407, 1973.

Schulz, M., and L. J. Lanzerotti, *Particle Diffusion in Radiation Belts,* Springer, New York, 1974.

Sellers, B., F. A. Hanser, and P. R. Morel, Design, fabrication and flight of a heavy particle identification instrument for satellites, *Rep. AFCRL-TR-73-0216,* Air Force Cambridge Res. Lab., Bedford, Mass., 1973.

Tinsley, B. A., Evidence that the recovery phase ring current consists of helium ions, *J. Geophys. Res., 81,* 6193, 1976.

Tverskoy, B. A., Transport and acceleration of charged particles in the earth's magnetosphere, *Geomagn. Aeron. USSR, 5,* Engl. Transl., 617, 1965.

Van Allen, J. A., and B. A. Randall, Evidence of direct durable capture of 1–8 MeV solar alpha particles onto geomagnetically trapped orbits, *J. Geophys. Res., 76,* 1830, 1971.

Walt, M., The radial diffusion of trapped particles induced by fluctuating magnetospheric fields, *Space Sci. Rev., 12,* 446, 1971.

(Received November 18, 1975;
accepted January 17, 1977.)

72-076B-01A
DSC # 430

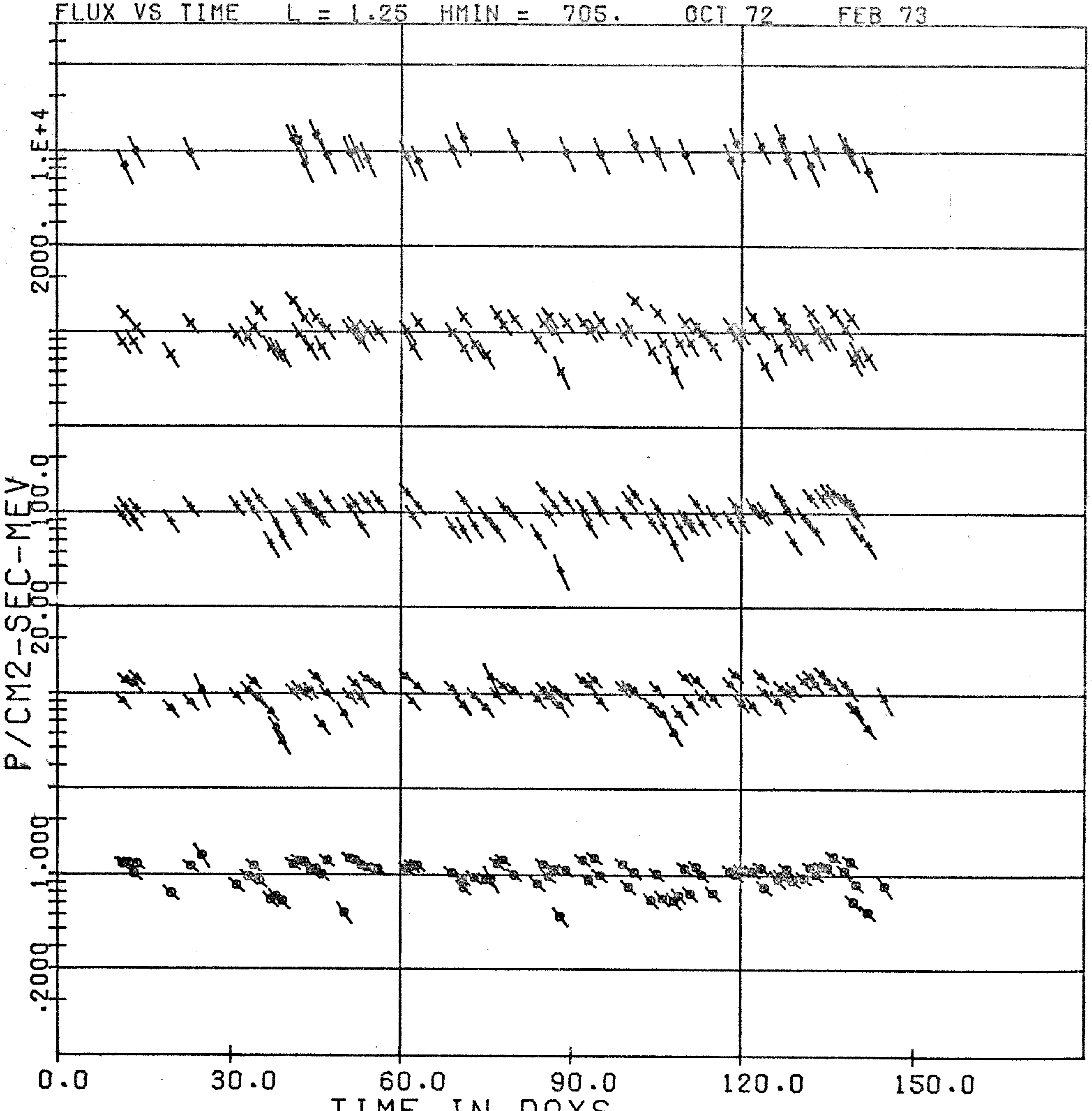

S72-1 OMNIDIRECTIONAL FLUXES.
CURVE AVGS 37.95, 41.01, 38.61, 43.25, 45.15
⊙ 36 MEV △ 23 MEV + 15 MEV × 9 MEV ◇ 6 MEV

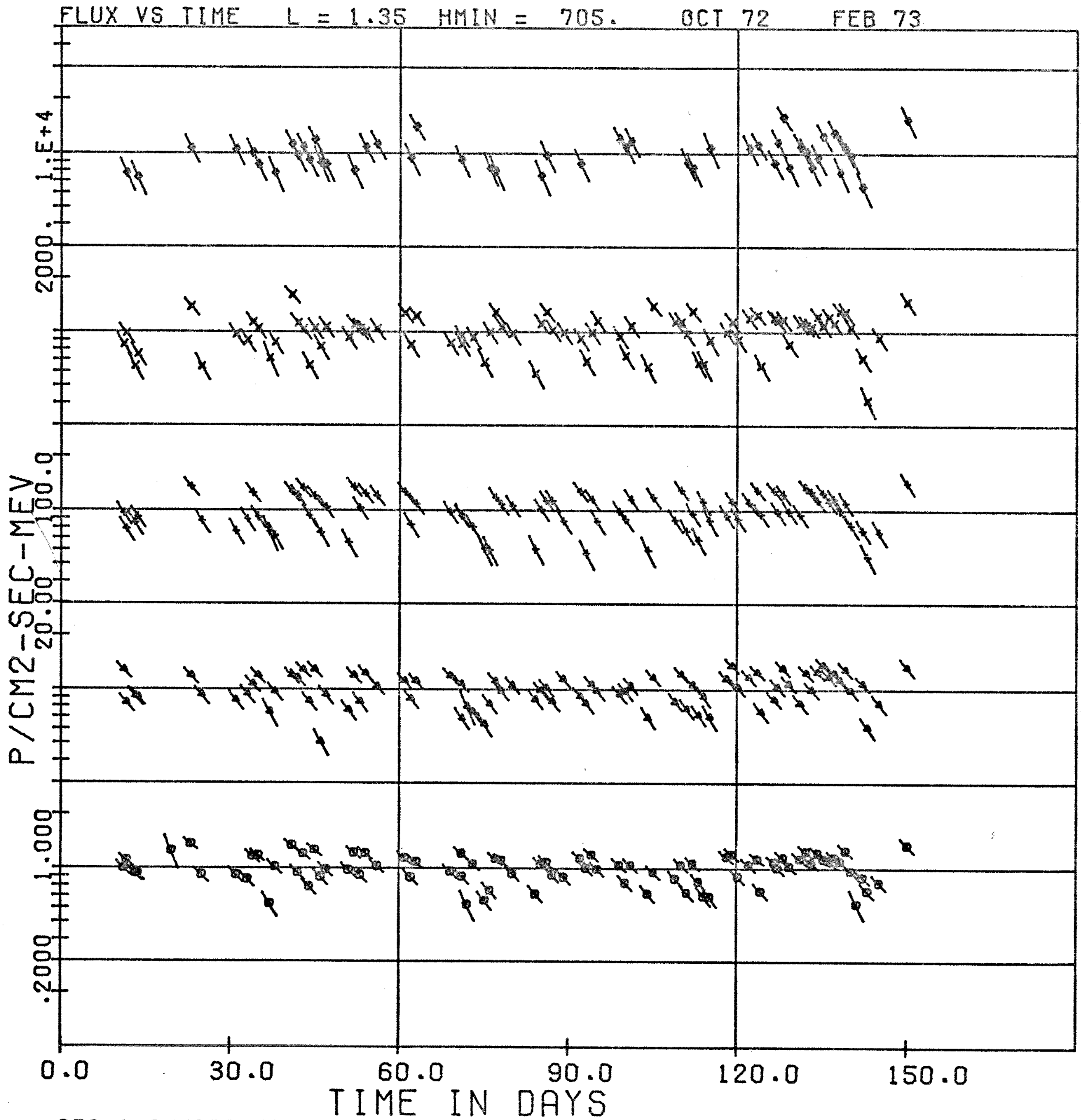

S72-1 OMNIDIRECTIONAL FLUXES.
CURVE AVGS 52.91, 60.79, 61.19, 78.23, 97.46
⊙ 36 MEV △ 23 MEV + 15 MEV × 9 MEV ◇ 6 MEV

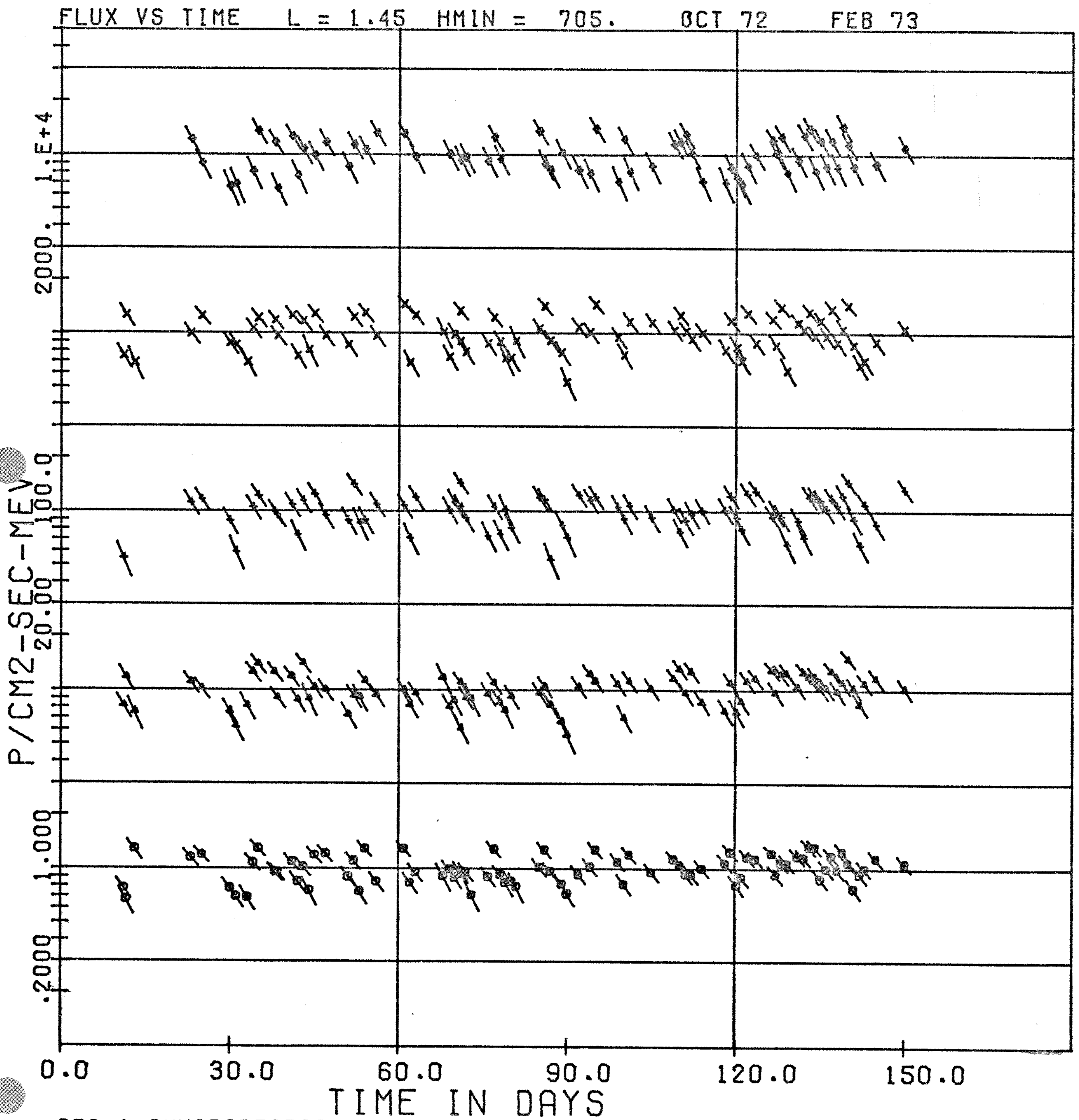

S72-1 OMNIDIRECTIONAL FLUXES.
CURVE AVGS 42.88. 50.49. 61.62. 109.50. 145.62
⊙ 36 MEV △ 23 MEV + 15 MEV × 9 MEV ◇ 6 MEV

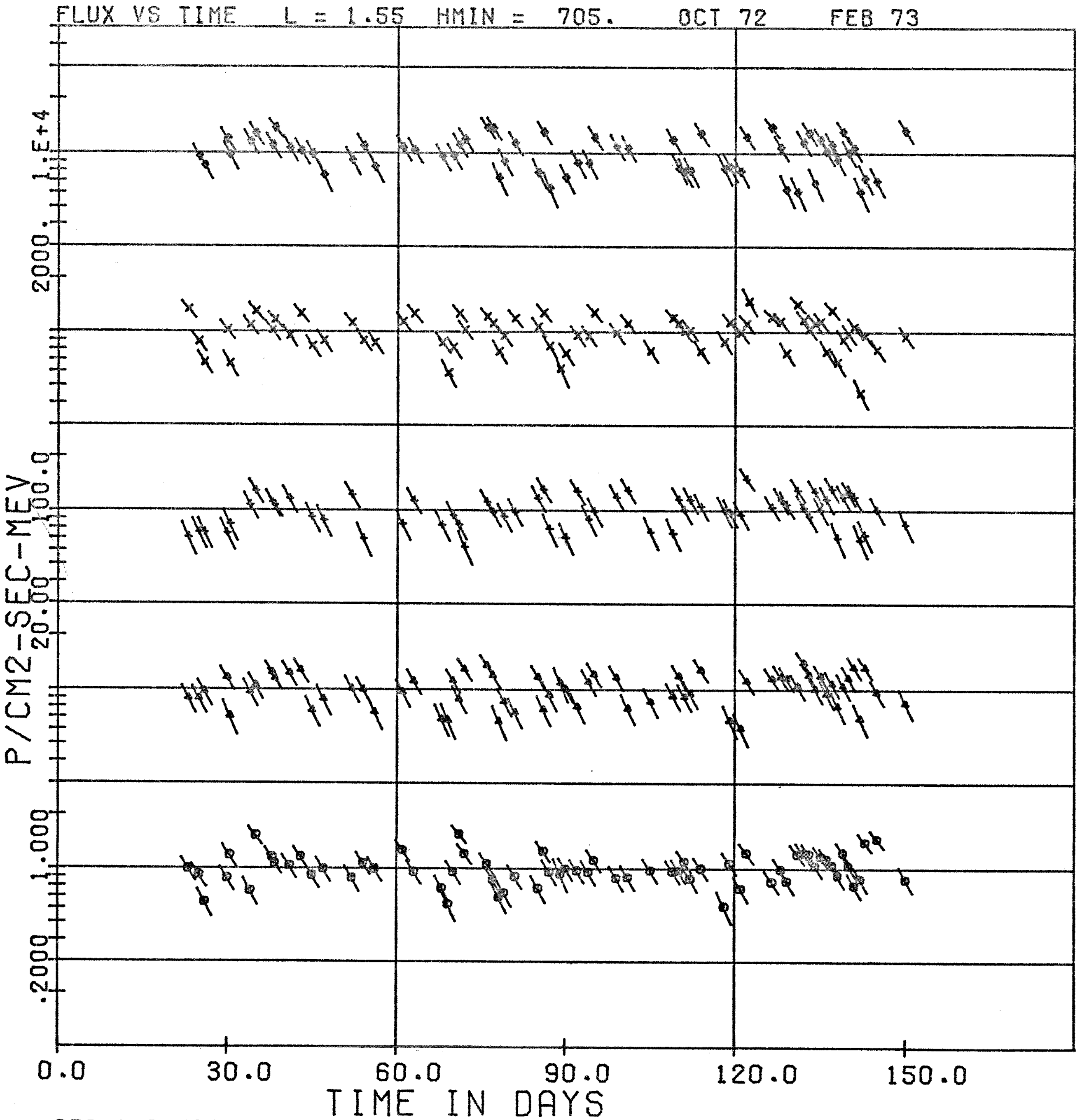

S72-1 OMNIDIRECTIONAL FLUXES.
CURVE AVGS 31.01. 42.06. 63.43. 144.88. 214.49
O 36 MEV △ 23 MEV + 15 MEV X 9 MEV ◇ 6 MEV

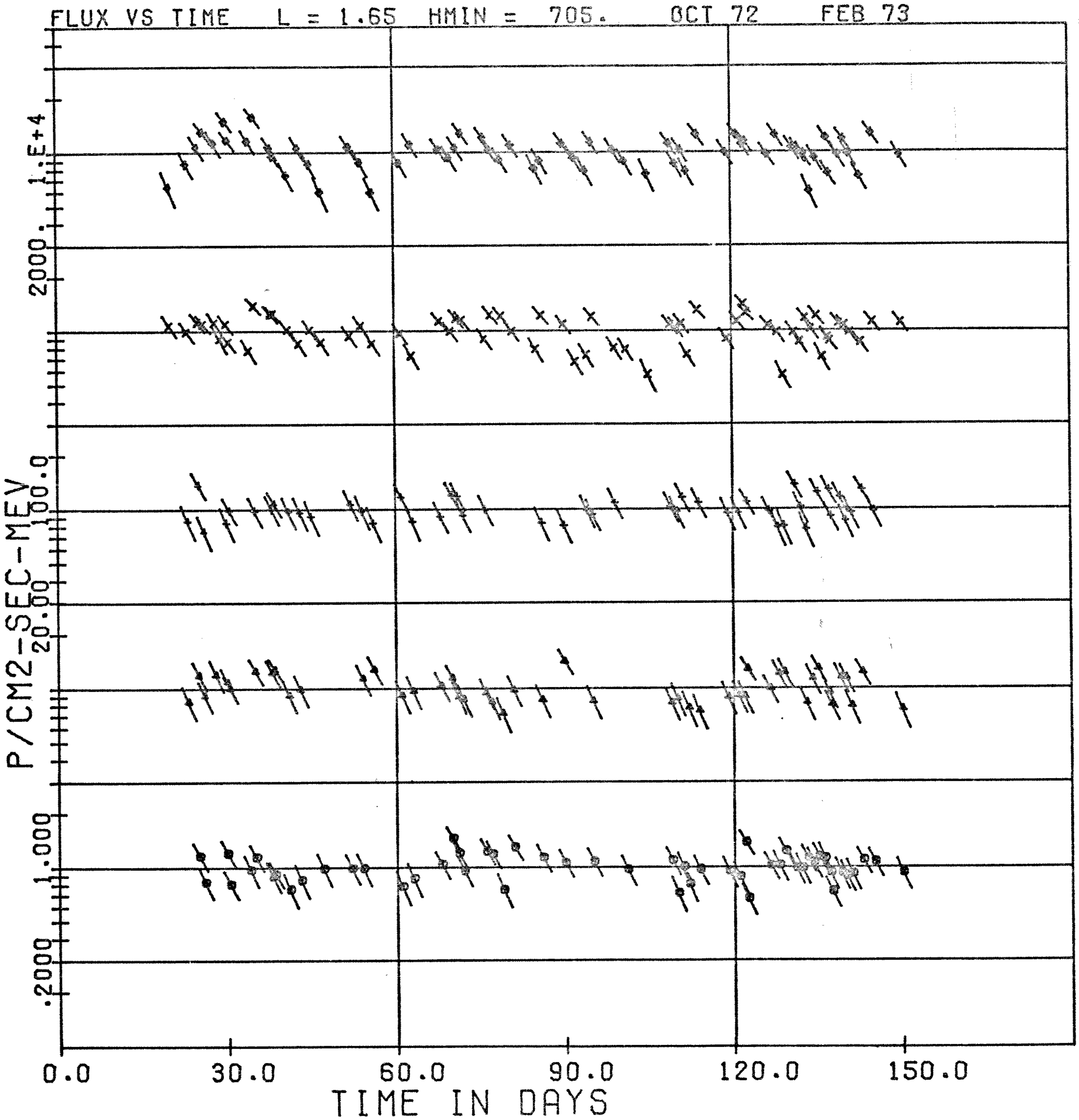

S72-1 OMNIDIRECTIONAL FLUXES.
CURVE AVGS 23.47, 38.56, 61.54, 171.74, 300.08
⊙ 36 MEV △ 23 MEV + 15 MEV × 9 MEV ◇ 6 MEV

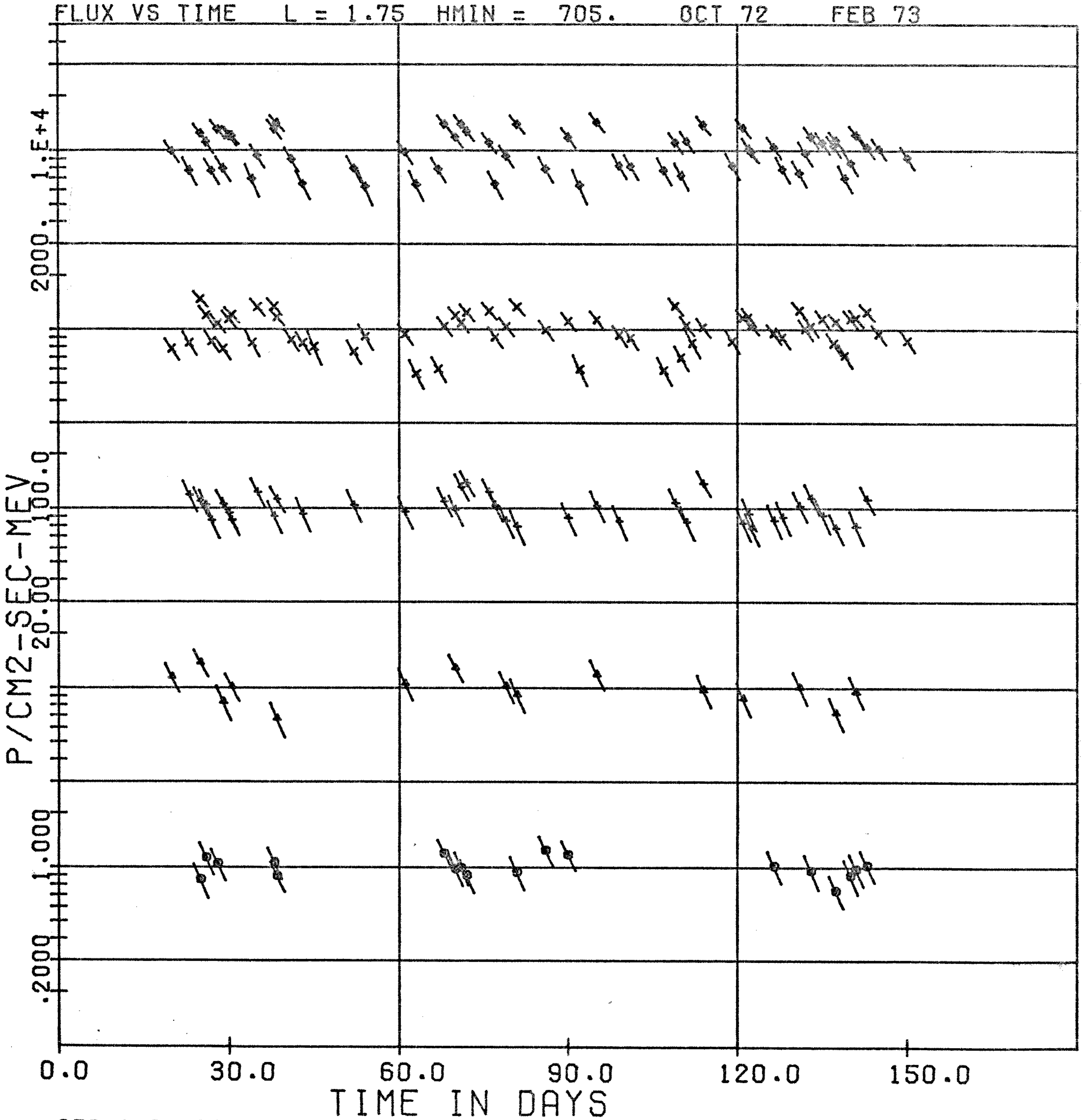

S72-1 OMNIDIRECTIONAL FLUXES.
CURVE AVGS 20.48, 36.46, 65.59, 184.24, 377.20
⊙ 36 MEV △ 23 MEV + 15 MEV × 9 MEV ◇ 6 MEV

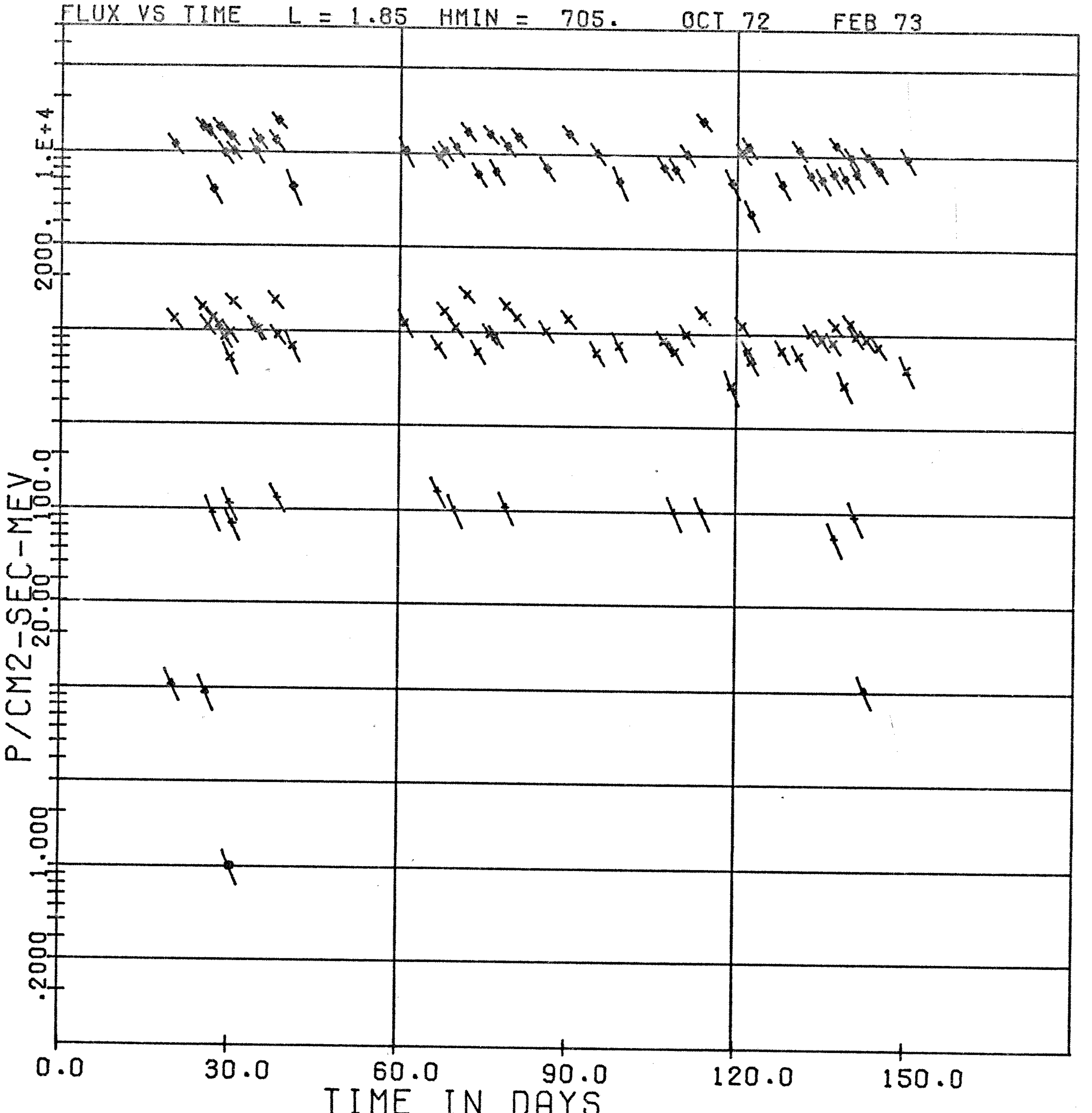

S72-1 OMNIDIRECTIONAL FLUXES.
CURVE AVGS 15.18, 37.61, 62.43, 194.35, 479.41
⊙ 36 MEV △ 23 MEV + 15 MEV × 9 MEV ◇ 6 MEV

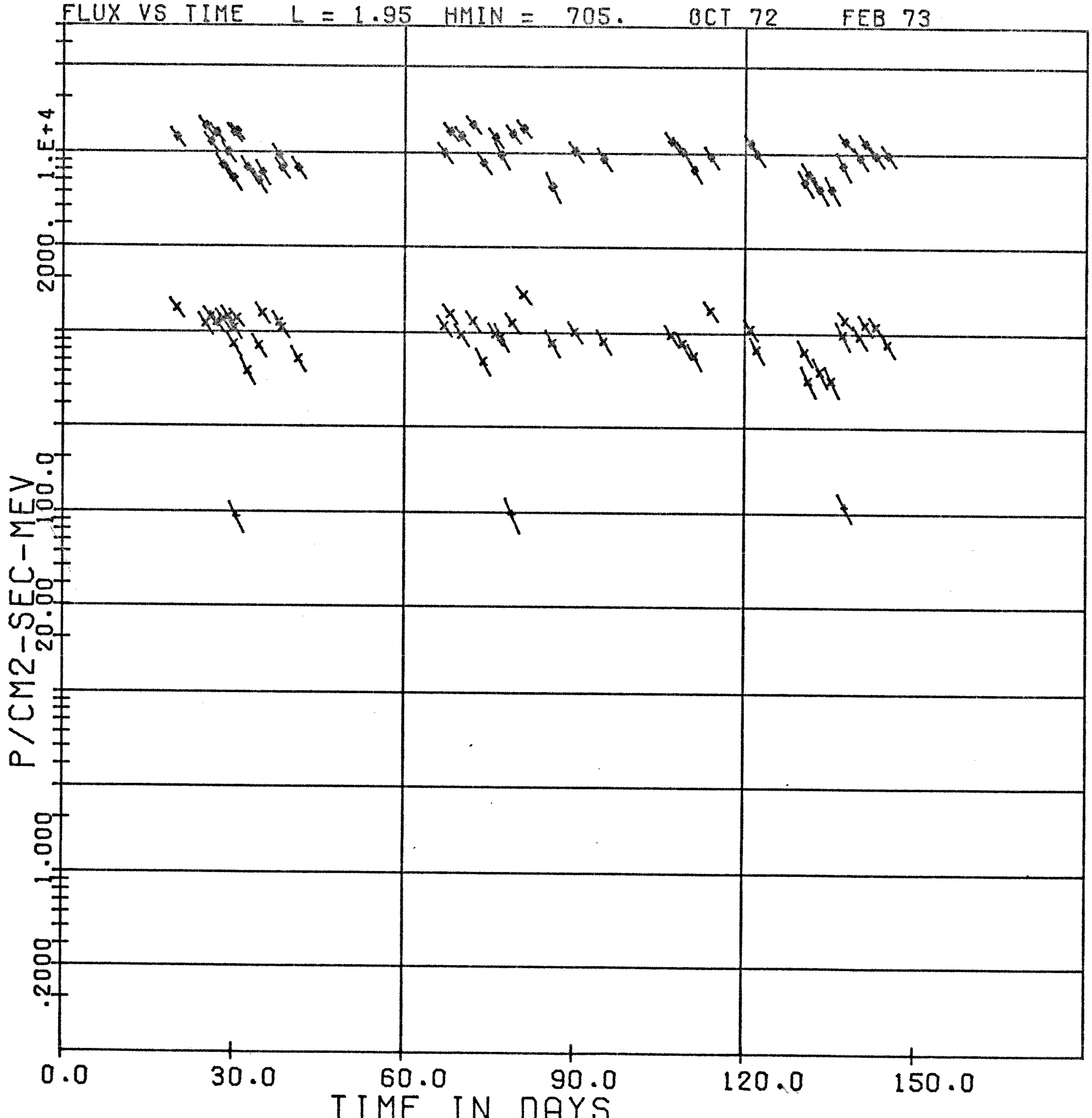

S72-1 OMNIDIRECTIONAL FLUXES.
CURVE AVGS 0.00. 0.00. 63.53. 180.46. 520.84
⊙ 36 MEV △ 23 MEV + 15 MEV × 9 MEV ◇ 6 MEV

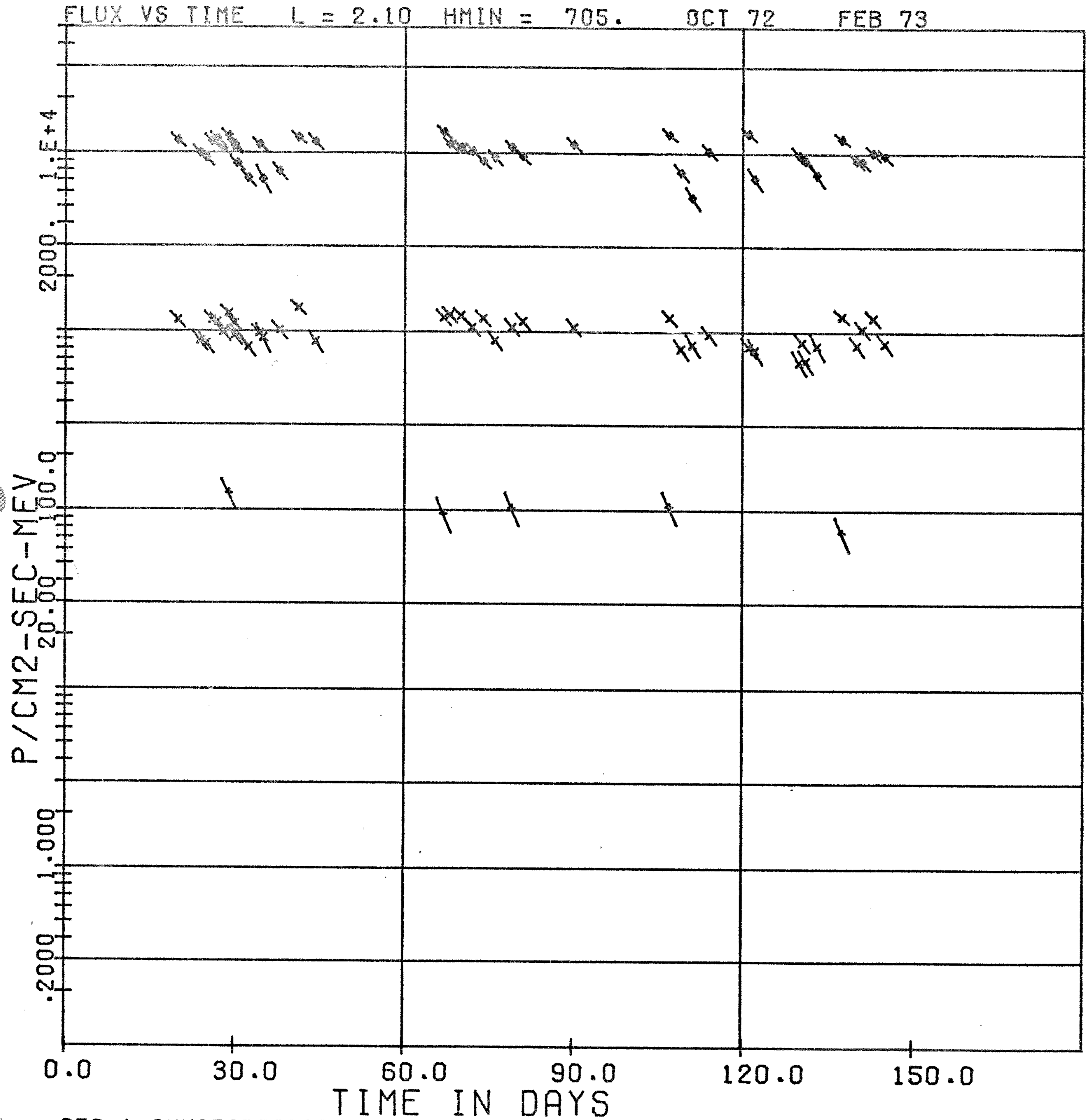

S72-1 OMNIDIRECTIONAL FLUXES.
CURVE AVGS 0.00. 0.00. 36.99. 156.27. 584.18
⊙ 36 MEV △ 23 MEV + 15 MEV × 9 MEV ◇ 6 MEV

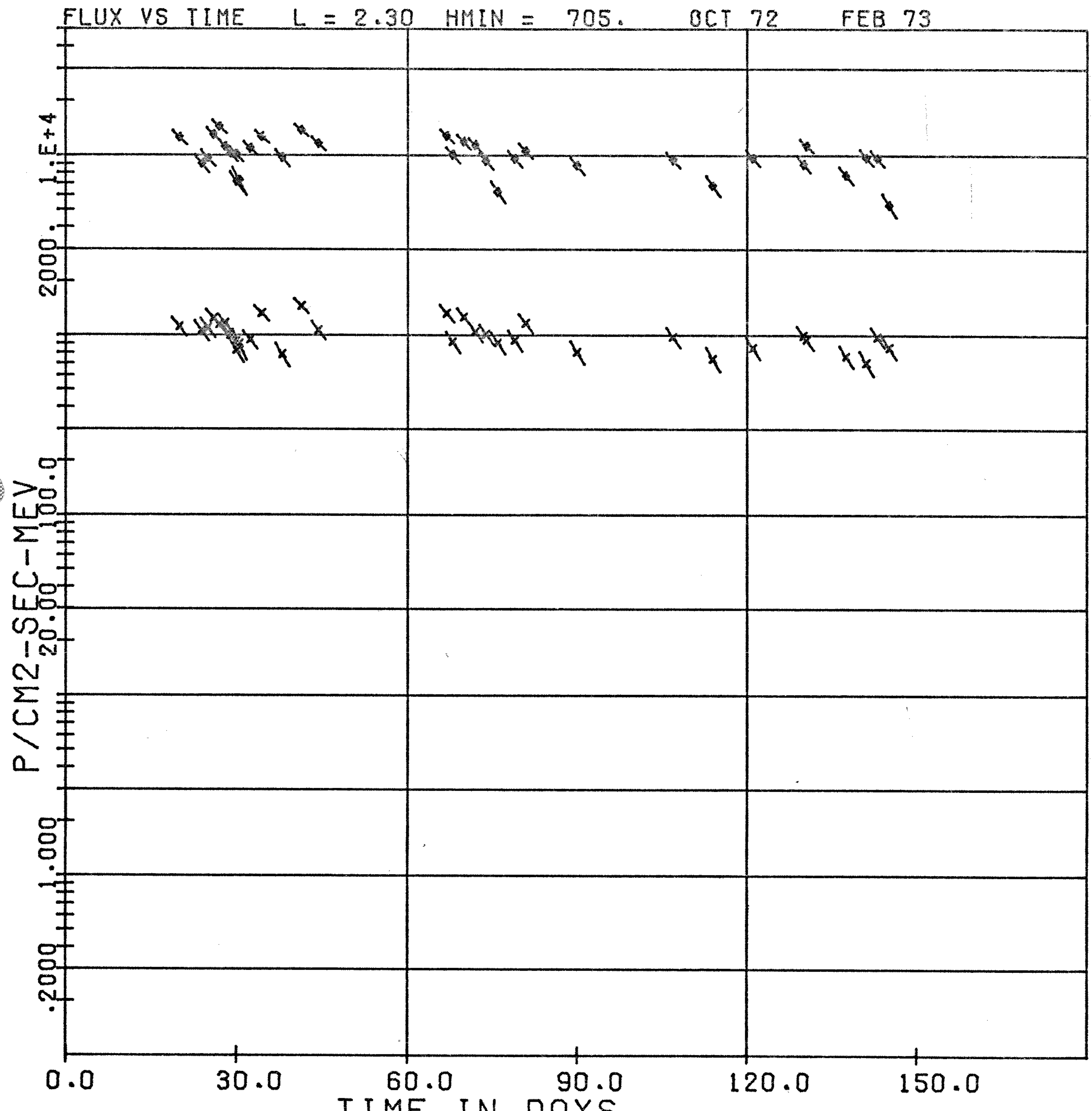

S72-1 OMNIDIRECTIONAL FLUXES.
CURVE AVGS 0.00, 0.00, 0.00, 143.39, 573.94
⊙ 36 MEV △ 23 MEV + 15 MEV × 9 MEV ◇ 6 MEV

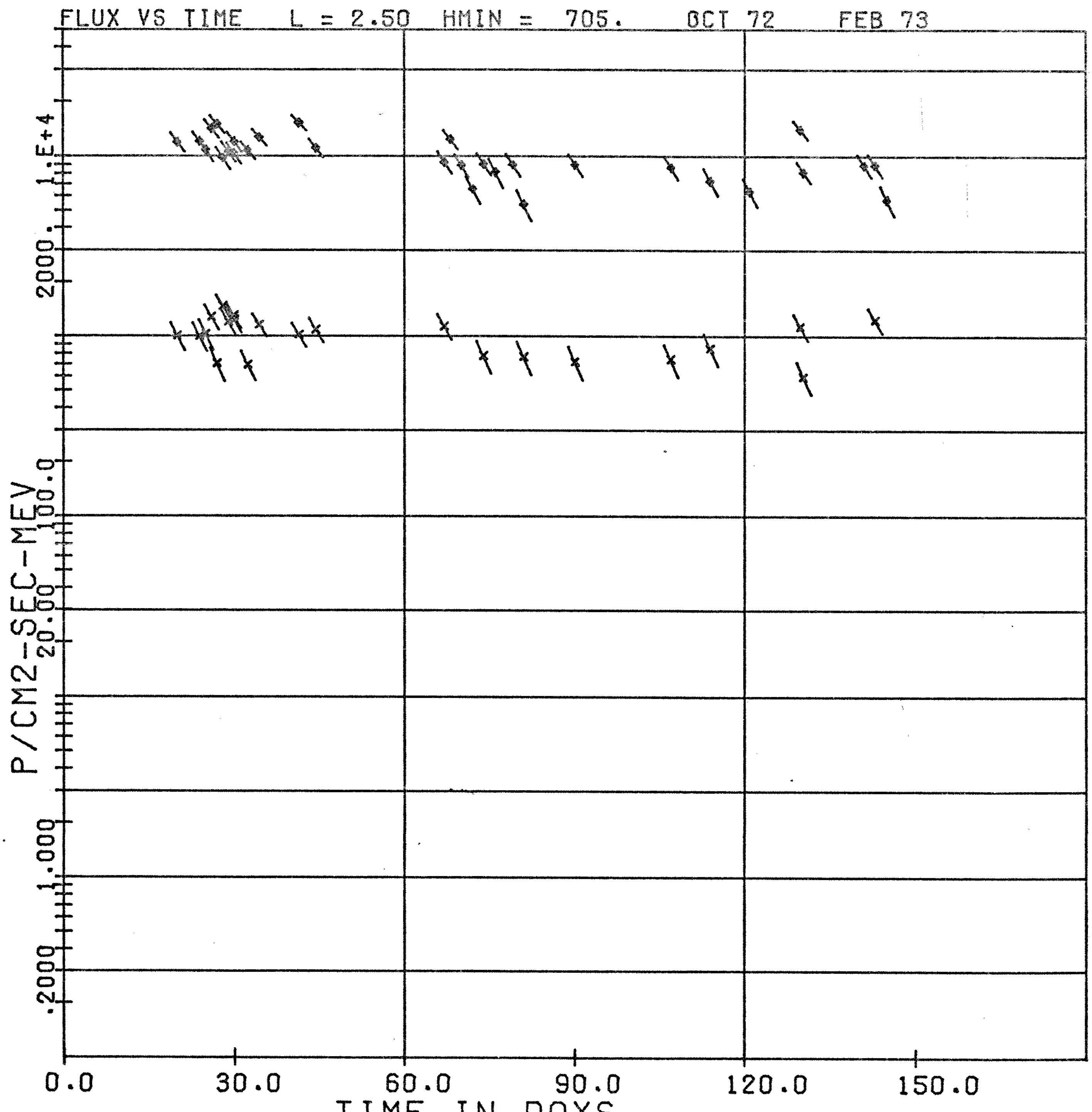

S72-1 OMNIDIRECTIONAL FLUXES.
CURVE AVGS 0.00, 0.00, 0.00, 86.82, 380.63
⊙ 36 MEV △ 23 MEV + 15 MEV X 9 MEV ◇ 6 MEV

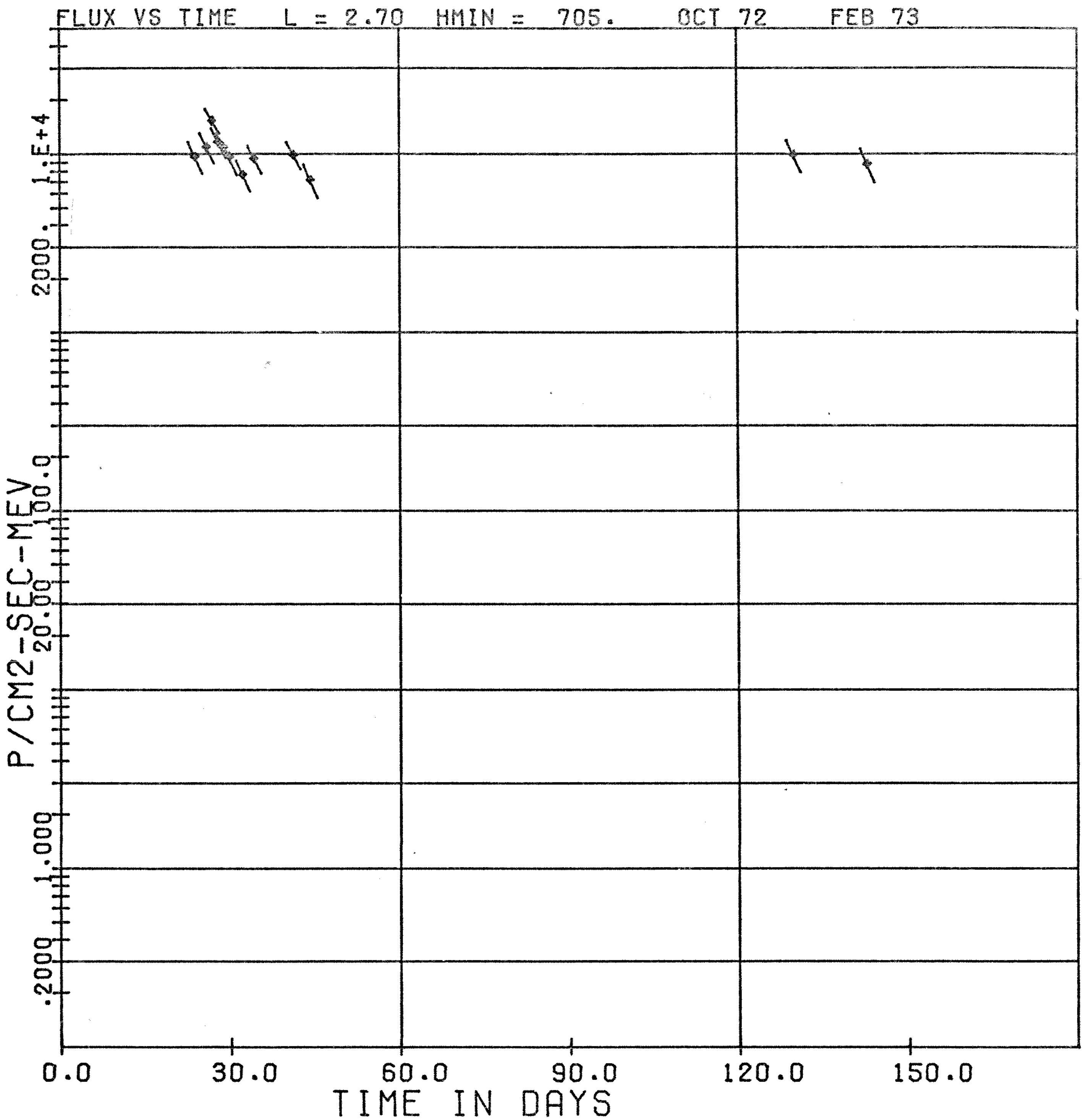

S72-1 OMNIDIRECTIONAL FLUXES.
CURVE AVGS 0.00. 0.00. 0.00. 0.00. 204.04
⊙ 36 MEV △ 23 MEV + 15 MEV × 9 MEV ◇ 6 MEV

Data Set Description:

The S72-1 "One-Degree Latitude-Longitude sort" data set is basically a sequential file containing 15600 logical records of 32 words each. Word thirty-two of each record is an index defining its relative position in the data set (ie the logical records were numbered from one to 15600). Each of the records corresponds to a one degree square of latitude and longitude. The follwing two fortran statements serve to define and illustrate this relationship;

```
XLAT=FLOAT(MOD(INDX-1),80)-69.5
XLONG=(INDX-1)/80 -139.5
```

where

XLAT is north geographic latitude

XLONG is east geographic longitude

INDX is the contents of word 32

FLOAT and MOD are standard fortran functions.

Hence INDX defines a one-to-one mapping of the data set onto the latitude longitude region $-70.0^{\circ} \leq$ XLAT $\leq 10.0^{\circ}$ north, $-140.0^{\circ} \leq$ XLONG $\leq 55.0^{\circ}$ east.

Pitch Angle and Energy Structure.

The first 30 words of a logical record correspond to the pitch angle intervals of width two degrees ($90.0^{\circ} - 88.0^{\circ}$) through ($32.0^{\circ} - 30.0^{\circ}$) respectively. Word thirty-one corresponds to the interval ($30.0^{\circ} - 0.0^{\circ}$). Each word contains six values in a packed format. The first five are the total observed counts for the five energy bins (45.0 Mev - 28.0 Mev), (28.0 - 18.2), (18.2 - 12.2), (12.2 - 7.0), (7.0 - 5.0). The sixth value is the total number of observations for that pitch angle interval and that latitude - longitude square. Each observation was of 0.08 seconds duration. The five counts were packed into nine consecutive bits each beginning at the left-most bit of the sixty bit CDC word and the number of observations was packed into the remaining fifteen bits.

Tape Version:

Since word 32 of each logical record identifies its place in the data set, the logical records where there were no observations could be dropped from the file to give a more compact version. This file was then blocked fifteen logical records per physical record with two prefix integers added to give an "auto-indexing" file and written to tape. All short records were blank filled to give a uniform 482 word block structure.

The tape VETTE3 contains five identical copies in this format to give a built in redundancy which should assure its readability.

Tape Description: Title: VETTE3

Tape type: 9-track; unlabeled

Density: ~~1600~~ 6250 BPI; phase encoded

Creation date: 23 May 78

Programmer: E. Holeman

No. of files: five

No. of records/file: app. 670

no of words/record: 482

Description of Contents:

VETTE3 contains five identical copies of the S72-1 "One-Degree Latitude Longitude sort" data set. Each copy contains ND + NB physical records where ND is the number of data records and NB is the number of "bookkeeping" records which identify the orbits making up the data set.

Record Structure:

All records, with the possible exception of records No. ND and ND + NB, have the basic structure:

IWORDS,JCOLS,((MATRIX(I,J),I=1,IWORDS),J=1,JCOLS)

where IWORDS = 32, JCOLS = 15 for the data records and IWORDS = 4, JCOLS = 120 for the bookkeeping records. Records ND and ND + NB may have a smaller value for JCOLS, and if so are blank filled to give a 482 word physical record.

Comments on Program OMSDJT.

Program OMSDJT is included in this package as an aide to your initial interpretation of the tape VETTE3. It reads each of the five copies of the data set and produces an identical output record for each consisting of an Omnidirectional Flux vs Latitude - Longitude table plus three check-sum tables confirming that all five copies are probably identical.

OMSDJT is CDC dependent and intended as an illustration only, hence no attempt was made to reduce it to ANSI standard fortran and no card deck copy was included in this package. Its comment sections are sparce but hopefully they will prove adequate. Internally, there are calls to four CDC system routines, OPENMS, READMS,WRITMS, AND ISBYTX. The first three form a random file system on the CDC mass storage disk. ISBYTX is the system bit manipulation routine which we use to pack and unpack the data in subroutine AADD. The interpretation of their usage is straight forward and should be apparent in context.

Flux Calculations.

The constants FXK1 and FXK2 are two constants required to compute flux rates from the data. FXK1 is the reciprical of the product of the instruments geometric factor and the time increment correspoiding to a single observation. (G = 0.0257 cm^2 ster and delta T = .08 sec) FXK2 is defined in terms of FXK1 in the program. We then define directional and omnidirectional flux for the kth energy channel to be:

$$Jdir = FXK1*(ND_k/NDOB_k)/DE_k$$

$$Jomni = FXK2*(NO_k/NOOB_k)/DE_k$$

where ND_k is the number of counts in the first pitch angle interval (90.0° - 88.0°), NO_k is the sum of the counts over all 31 pitch angle intervals, $NDOB_k$ is the number of observations for the first pitch angle interval, $NOOB_k$ is the sum of observations over all 31 pitch angles, and DE_k is the appropriate delta-Energy. Note that the enclosed Omnidirectional Flux Tables are not complete in the sense that "latitude lines" where there were observations but no counts were deleted. Hence a sum over the number of observations column will not necessarily agree with the number in the one page Longitude Summary at the end.

```
      PROGRAM OMSDJT(UFILE,TAPE8,OUTPUT,TAPE1=UFILE,TAPE6=
     +OUTPUT)
C***********************************************************************
C*****
C 1978    PROGRAM.  E. HOLEMAN.  LAST ALTERATION  23 MAY 78
C 1978    THIS PROGRAM WAS WRITTEN AS PART OF THE DOCUMENTATION
C 1978    PACKAGE BEING PREPARED FOR TRANSMISSION TO VETTE
C         AND A COPY OF IT WILL ACCOMPANY THE TAPE CONTAINING
C         THE S72-1 ONE DEGREE LATITUDE LONGITUDE PITCH-ANGLE
C         SORTED DATA.
C*****
C  PROGRAM COMPACTS THE 1 DEGREE LATITUDE - LONGITUDE SORTED
C  DATA FILE INTO A 5 DEGREE FORMAT AND LISTS VARIOUS SUMMARIES.
C
C  ITS PURPOSE IS TO PRODUCE A SET OF CHECK-SUM TYPE SUMMARIES
C  WHICH MAY BE USED TO DETERMINE WHETHER THE ONE-DEGREE TAPE
C  HAS BEEN READ SUCCESSFULLY AND THE DATA UNPACKED PROPERLY.
C*****
C  APPROXIMATE FIELD LENGTH REQUIRED IS 43600 WORDS.
C*****
C***********************************************************************
C*****
      DIMENSION JDT(32,15),IRF(32,16),INDX(40),FX(6),DFX(6),DE(5),
     +JADD(5),IADD(5),KSY(7,31),LSY(7,16),MSY(7),NSY(7,2),MSYA(7)
      DATA DE /17.,9.8,5.,5.2,2.,40.7
      PI=3.14159265+
      FXK1=466.3613
      FXK2=4.*PI*(PI/2.)*FXK1
      NFIL=0
      REWIND1
      CALL OPENMS(8,INDX,40,0)
  230 CONTINUE
      DO 240 II=1,16
      DO 240 JJ=1,32
      IRF(JJ,II)=0
  240 CONTINUE
      DO 10 II=1,39
      CALL WRITMS(8,IRF,512,II,-1)
   10 CONTINUE
      JJL=39
      T1=SECOND(TTI)
      ADTT=DATE(ZZZ)
      ATIM=TIME(ZZZ)
      NFIL=NFIL+1
      WRITE(6,2001) ADTT,ATIM,NFIL
 2001 FORMAT(1H1,4X,*S72-1 PROCESSING BEGUN IN OMSDJ*,5X,A10,5X,
     +A10,*  FILE NO.*,I3)
C
C*****
C  READ UFILE DATA AND COPY TO RANDOM FILE.
C*****
      IFGA=0
      IFGD=0
   20 CONTINUE
      READ(1) I1,I2,JDT
      IF(EOF(1)) 70,30
   30 CONTINUE
```

```
      ICK=I1*I2
      IF(ICK.LT.4.OR.ICK.GT.480) GO TO 20
      IFGA=0
      IFGC=1
      IF(I1.NE.32) GO TO 20
      DO 60 II=1,I2
      IF(JDT(32,II).LT.1.OR.JDT(32,II).GT.15600) GO TO 60
      II1=(JDT(32,II)-1)/400+1
      IF(II1.NE.JJL) CALL WRITMS(8,IRF,512,JJL,-1)
      IF(II1.NE.JJL) CALL READMS(8,IRF,512,II1)
      JJL=II1
      II2=MOD(JDT(32,II)-1,80)/5+1
      DO 50 JJ=1,31
      CALL DADD(IRF(JJ,II2),IADD,NOBS)
      CALL DADD(JDT(JJ,II),JADD,MOBS)
      DO 40 KK=1,5
      IADD(KK)=IADD(KK)+JADD(KK)
   40 CONTINUE
      NOBS=NOBS+MOBS
      CALL AADD(IRF(JJ,II2),IADD,NOBS)
   50 CONTINUE
      IRF(32,II2)=(II1-1)*16+II2
   60 CONTINUE
      GO TO 20
   70 CONTINUE
      IFGA=IFGA+1
      IF(IFGA.EQ.3) GO TO 250
      IF(IFGC.EQ.0) GO TO 20
C
C*****
C  INPUT COMPLETE.  GENERATE SUMMARIES.
C  PRINT OUT FLUX VS PITCH-ANGLE TABLE FOR EACH LAT-LONG
C*****
      CALL WRITMS(8,IRF,512,JJL,-1)
      DO 110 II=1,39
      MSY(1)=MSY(2)=MSY(3)=MSY(4)=MSY(5)=MSY(6)=MSY(7)=0
      CALL READMS(8,IRF,512,II)
      XLG=FLOAT(5*II)+217.5
      IF(XLG.GT.360.) XLG=XLG-360.
      IFGB=1
      DO 110 JJ=1,16
      IF(IRF(32,JJ).LT.1) GO TO 110
      XLT=-72.5+FLOAT(5*JJ)
      IF(IFGB.EQ.1) WRITE(6,2002) XLG
 2002 FORMAT(///1X,*OMNIDIRECTIONAL FLUX SUMMARY VS LATITUDE FOR*
     +* LONGITUDE=*,F7.1/* LAT + 5 ENERGIES WITH RMS ERROR + NO OF*
     +* OBS + LINE TOTALS*)
      IFGB=0
      MSYA(1)=MSYA(2)=MSYA(3)=MSYA(4)=MSYA(5)=MSYA(6)=MSYA(7)=0
      DO 90 KK=1,31
      CALL DADD(IRF(KK,JJ),IADD,NOBS)
      DO 80 LL=1,5
      MSY(6)=MSY(6)+IADD(LL)
      MSY(LL)=MSY(LL)+IADD(LL)
      MSYA(6)=MSYA(6)+IADD(LL)
      MSYA(LL)=MSYA(LL)+IADD(LL)
   80 CONTINUE
```

```
      MSY(7)=MSY(7)+NOBS
      MSYA(7)=MSYA(7)+NOBS
   90 CONTINUE
      DO 100 KK=1,6
      DFX(KK)=0.
      FX(KK)=FLOAT(MSYA(KK))/DE(KK)/FLOAT(MSYA(7))*FXK2
      IF(MSYA(KK).LT.1) GO TO 100
      DFX(KK)=FX(KK)/SQRT(FLOAT(MSYA(KK)))
  100 CONTINUE
      WRITE(6,2003) XLT,(FX(I),DFX(I),I=1,5),MSYA(7),FX(6),DFX(6)
 2003 FORMAT(1X,F5.1,5(F8.2,F6.2),I6,F8.2,F6.2)
  110 CONTINUE
C
C*****
C  WRITE SUMMARY OF LONGITUDE DISTRIBUTION.
C  DO THE CROSS SUMMING FOR PITCH ANGLE AND LATITUDE SUMMARIES.
C*****
      WRITE(6,2001) ADTT,ATIM,NFIL
      WRITE(6,2004)
 2004 FORMAT(1X,*LONGITUDE SUMMARY*/1X,*LONG + 5 ENERGIES + *
     +*NO OF OBS + LINE TOTAL*)
      DO 120 II=1,7
      DO 120 JJ=1,31
      KSY(II,JJ)=0
      IF(JJ.GT.16) GO TO 120
      LSY(II,JJ)=0
  120 CONTINUE
      NSY(1,2)=NSY(2,2)=NSY(3,2)=NSY(4,2)=NSY(5,2)=NSY(6,2)=NSY(7,2)=0
      DO 160 II=1,39
      XL=FLOAT(II*5)+217.5
      IF(XL.GT.360.) XL=XL-360.
      CALL READMS(8,IRF,512,II)
      NSY(1,1)=NSY(2,1)=NSY(3,1)=NSY(4,1)=NSY(5,1)=NSY(6,1)=NSY(7,1)=0
      DO 140 JJ=1,16
      IF(IRF(32,JJ).LT.0) GO TO 140
      DO 130 KK=1,31
      CALL DADD(IRF(KK,JJ),IADD,NOBS)
      KSY(6,KK)=KSY(6,KK)+NOBS
      LSY(6,JJ)=LSY(6,JJ)+NOBS
      NSY(6,1)=NSY(6,1)+NOBS
      DO 130 LL=1,5
      KSY(LL,KK)=KSY(LL,KK)+IADD(LL)
      LSY(LL,JJ)=LSY(LL,JJ)+IADD(LL)
      NSY(LL,1)=NSY(LL,1)+IADD(LL)
      NSY(7,1)=NSY(7,1)+IADD(LL)
  130 CONTINUE
  140 CONTINUE
      IF(NSY(6,1).LT.1) GO TO 160
      WRITE(6,2005) XL,(NSY(I,1),I=1,7)
 2005 FORMAT(1X,F5.1,5I7,2I10)
      DO 150 KK=1,7
      NSY(KK,2)=NSY(KK,2)+NSY(KK,1)
  150 CONTINUE
  160 CONTINUE
      XL=0.
      WRITE(6,2005) XL,(NSY(I,2),I=1,7)
C
```

```
C*****
C  WRITE SUMMARY OF PITCH ANGLE DISTRIBUTION.
C*****
      WRITE(6,2001) ADTT,ATIM,NFIL
      WRITE(6,2006)
 2006 FORMAT(1X,*PITCH ANGLE SUMMARY*/1X,*PA + 5 ENERGIES + *
     +*NO OF OBS + LINE TOTAL*)
      DO 190 II=1,31
      DO 170 JJ=1,5
      KSY(7,II)=KSY(7,II)+KSY(JJ,II)
  170 CONTINUE
      ID=91-2*II
      WRITE(6,2007) ID,(KSY(I,II),I=1,7)
 2007 FORMAT(1X,I3,5I7,2I10)
      IF(II.EQ.1) GO TO 190
      DO 180 JJ=1,7
      KSY(JJ,1)=KSY(JJ,1)+KSY(JJ,II)
  180 CONTINUE
  190 CONTINUE
      ID=0
      WRITE(6,2007) ID,(KSY(I,1),I=1,7)
C
C*****
C  WRITE SUMMARY OF LATITUDE DISTRIBUTION
C*****
      WRITE(6,2001) ADTT,ATIM,NFIL
      WRITE(6,2008)
 2008 FORMAT(1X,*LAT SUMMARY*/1X,*LAT + 5 ENERGIES + NO OF OBS + *
     +*LINE TOTAL*)
      DO 220 II=1,16
      DO 200 JJ=1,5
      LSY(7,II)=LSY(7,II)+LSY(JJ,II)
  200 CONTINUE
      XL=FLOAT(II*5)-72.5
      IF(LSY(6,II).GT.0) WRITE(6,2005) XL,(LSY(I,II),I=1,7)
      IF(II.EQ.1) GO TO 220
      DO 210 JJ=1,7
      LSY(JJ,1)=LSY(JJ,1)+LSY(JJ,II)
  210 CONTINUE
  220 CONTINUE
      XL=0.
      WRITE(6,2005) XL,(LSY(I,1),I=1,7)
      T1=SECOND(TT)-T1
      WRITE(6,2009) T1
 2009 FORMAT(1X,*END OF FILE ON OMSDJ*/1X,*OMSDJ PROCESSING *
     +*TIME*,F10.3)
      GO TO 230
  250 CONTINUE
      END
```

REFERENCE MAP (R=3)

```
      SUBROUTINE AADD(JCD,IADD,NADD)
C*****************************************************************
C*****
C  AADD IMPLIES ENCODE IADD,NADD INTO 1-WORD COMPOSITE
C*****
C  DADD IMPLIES DECODE 1-WORD COMPOSITE INTO IADD,NADD
C*****
C*****************************************************************
      DIMENSION IADD(5),JCD(2)
C*****
C  ENCODE 1-WORD COMPOSITE
C*****
      DO 10 II=1,4
      IF(IADD(II).GT.511) GO TO 20
   10 CONTINUE
      IF(IADD(5).GT.32767) GO TO 20
      JCD(1)=0B
      JCD(1)=ISBYTX(52,9,JCD(1),IADD(1))
      JCD(1)=ISBYTX(43,9,JCD(1),IADD(2))
      JCD(1)=ISBYTX(34,9,JCD(1),IADD(3))
      JCD(1)=ISBYTX(25,9,JCD(1),IADD(4))
      JCD(1)=ISBYTX(16,9,JCD(1),IADD(5))
      JCD(1)=ISBYTX(1,15,JCD(1),NADD)
      RETURN
C******
C  DECODE 1-WORD COMPOSITE
C****
      ENTRY DADD
      IADD(1)=IADD(2)=IADD(3)=IADD(4)=IADD(5)=0B
      IADD(1)=SHIFT(JCD(1),9).AND.777B
      IADD(2)=SHIFT(JCD(1).AND.777000000000000000B,-42)
      IADD(3)=SHIFT(JCD(1).AND.777000000000000B,-33)
      IADD(4)=SHIFT(JCD(1).AND.777000000000B,-24)
      IADD(5)=SHIFT(JCD(1).AND.777000000B,-15)
      NADD=JCD(1).AND.77777B
      RETURN
   20 CONTINUE
      WRITE(6,2001)
 2001 FORMAT(1X,*AADD SUBROUTINE OVERFLOW*)
      RETURN
      END
```

```
REFERENCE MAP (R=3)

DEF LINE    REFERENCES
    1         24
   28         36        40

N  TYPE              RELOCATION
 INTEGER      ARRAY     F.P.          REFS        9          14         16        18
                                       22     DEFINED        1         5*29       30
                                       34
 INTEGER                              REFS       14     DEFINED         13
```

P72. PROCESSING BEGUN IN OMSOJ 06/07/78 15.14.32. FILE NO. 1

OMNIDIRECTIONAL FLUX SUMMARY VS LATITUDE FOR LONGITUDE= 222.5

LAT + 5 ENERGIES WITH RMS ERROR + NO OF OBS + LINE TOTALS

-7.5	0.00	0.00	0.00	0.00	0.00	0.00	0.00	0.00	0.00	0.00	9168	0.00	0.00
-2.5	0.00	0.00	.07	.07	.33	.19	0.00	0.00	0.00	0.00	14628	.07	.03
2.5	0.00	0.00	0.00	0.00	0.00	0.00	0.00	0.00	0.00	0.00	10776	0.00	0.00

OMNIDIRECTIONAL FLUX SUMMARY VS LATITUDE FOR LONGITUDE= 227.5

LAT + 5 ENERGIES WITH RMS ERROR + NO OF OBS + LINE TOTALS

-12.5	0.00	0.00	0.00	0.00	0.00	0.00	0.00	0.00	0.00	0.00	1596	0.00	0.00
-7.5	0.00	0.00	0.00	0.00	0.00	0.00	0.00	0.00	0.00	0.00	14664	0.00	0.00
-2.5	0.00	0.00	0.00	0.00	0.00	0.00	0.00	0.00	0.00	0.00	14784	0.00	0.00
2.5	0.00	0.00	0.00	0.00	0.00	0.00	0.00	0.00	0.00	0.00	10128	0.00	0.00

OMNIDIRECTIONAL FLUX SUMMARY VS LATITUDE FOR LONGITUDE= 232.5

LAT + 5 ENERGIES WITH RMS ERROR + NO OF OBS + LINE TOTALS

-12.5	0.00	0.00	0.00	0.00	0.00	0.00	0.00	0.00	0.00	0.00	7920	0.00	0.00
-7.5	0.00	0.00	0.00	0.00	0.00	0.00	0.00	0.00	0.00	0.00	15744	0.00	0.00
-2.5	0.00	0.00	0.00	0.00	0.00	0.00	0.00	0.00	0.00	0.00	18216	0.00	0.00
2.5	0.00	0.00	0.00	0.00	0.00	0.00	0.00	0.00	0.00	0.00	10104	0.00	0.00

OMNIDIRECTIONAL FLUX SUMMARY VS LATITUDE FOR LONGITUDE= 237.5

LAT + 5 ENERGIES WITH RMS ERROR + NO OF OBS + LINE TOTALS

-17.5	0.00	0.00	0.00	0.00	0.00	0.00	0.00	0.00	0.00	0.00	612	0.00	0.00
-12.5	0.00	0.00	0.00	0.00	0.00	0.00	0.00	0.00	0.00	0.00	15228	0.00	0.00
-7.5	.03	.03	0.00	0.00	0.00	0.00	0.00	0.00	0.00	0.00	16740	.01	.01
-2.5	0.00	0.00	0.00	0.00	0.00	0.00	0.00	0.00	0.00	0.00	16896	0.00	0.00
2.5	0.00	0.00	0.00	0.00	0.00	0.00	0.00	0.00	0.00	0.00	7716	0.00	0.00

OMNIDIRECTIONAL FLUX SUMMARY VS LATITUDE FOR LONGITUDE= 242.5

LAT + 5 ENERGIES WITH RMS ERROR + NO OF OBS + LINE TOTALS

-17.5	0.00	0.00	0.00	0.00	0.00	0.00	0.00	0.00	0.00	0.00	6300	0.00	0.00
-12.5	.03	.03	0.00	0.00	0.00	0.00	0.00	0.00	0.00	0.00	18120	.01	.01
-7.5	0.00	0.00	0.00	0.00	0.00	0.00	0.00	0.00	0.00	0.00	22476	0.00	0.00
-2.5	0.00	0.00	0.00	0.00	0.00	0.00	0.00	0.00	0.00	0.00	22663	0.00	0.00
2.5	0.00	0.00	0.00	0.00	0.00	0.00	0.00	0.00	0.00	0.00	8052	0.00	0.00

OMNIDIRECTIONAL FLUX SUMMARY VS LATITUDE FOR LONGITUDE= 247.5
LAT + 5 ENERGIES WITH RMS ERROR + NO OF OBS + LINE TOTALS

-22.5	0.00	0.00	0.00	0.00	0.00	0.00	0.00	0.00	0.00	0.00	264	0.00	0.00
-17.5	0.00	0.00	0.00	0.00	0.00	0.00	0.00	0.00	0.00	0.00	17304	0.00	0.00
-12.5	0.00	0.00	0.00	0.00	0.00	0.00	0.00	0.00	0.00	0.00	18792	0.00	0.00
-7.5	0.00	0.00	0.00	0.00	0.00	0.00	0.00	0.00	0.00	0.00	15359	0.00	0.00
-2.5	0.00	0.00	0.00	0.00	0.00	0.00	0.00	0.00	0.00	0.00	15456	0.00	0.00
2.5	0.00	0.00	0.00	0.00	0.00	0.00	0.00	0.00	0.00	0.00	4955	0.00	0.00

OMNIDIRECTIONAL FLUX SUMMARY VS LATITUDE FOR LONGITUDE= 252.5
LAT + 5 ENERGIES WITH RMS ERROR + NO OF OBS + LINE TOTALS

-67.5	0.00	0.00	0.00	0.00	0.00	0.00	0.00	0.00	0.00	0.00	276	0.00	0.00
-22.5	0.00	0.00	0.00	0.00	0.00	0.00	0.00	0.00	0.00	0.00	6888	0.00	0.00
-17.5	0.00	0.00	0.00	0.00	0.00	0.00	0.00	0.00	0.00	0.00	11983	0.00	0.00
-12.5	0.00	0.00	.07	.07	0.00	0.00	0.00	0.00	0.00	0.00	13452	.02	.02
-7.5	0.00	0.00	0.00	0.00	0.00	0.00	0.00	0.00	0.00	0.00	13236	0.00	0.00
-2.5	0.00	0.00	0.00	0.00	0.00	0.00	0.00	0.00	0.00	0.00	15288	0.00	0.00
2.5	0.00	0.00	0.00	0.00	0.00	0.00	0.00	0.00	0.00	0.00	3120	0.00	0.00

OMNIDIRECTIONAL FLUX SUMMARY VS LATITUDE FOR LONGITUDE= 257.5
LAT + 5 ENERGIES WITH RMS ERROR + NO OF OBS + LINE TOTALS

-67.5	1.05	1.05	0.00	0.00	0.00	0.00	0.00	0.00	0.00	0.00	540	.44	.44
-37.5	0.00	0.00	0.00	0.00	0.00	0.00	0.00	0.00	0.00	0.00	204	0.00	0.00
-27.5	0.00	0.00	0.00	0.00	0.00	0.00	0.00	0.00	0.00	0.00	3528	0.00	0.00
-22.5	0.00	0.00	0.00	0.00	0.00	0.00	0.00	0.00	0.00	0.00	11916	0.00	0.00
-17.5	.04	.04	0.00	0.00	0.00	0.00	0.00	0.00	0.00	0.00	12624	.02	.02
-12.5	.05	.05	0.00	0.00	0.00	0.00	0.00	0.00	0.00	0.00	11616	.02	.02
-7.5	0.00	0.00	0.00	0.00	0.00	0.00	0.00	0.00	0.00	0.00	12912	0.00	0.00
-2.5	0.00	0.00	0.00	0.00	0.00	0.00	0.00	0.00	0.00	0.00	10740	0.00	0.00
2.5	0.00	0.00	0.00	0.00	0.00	0.00	0.00	0.00	0.00	0.00	1020	0.00	0.00

OMNIDIRECTIONAL FLUX SUMMARY VS LATITUDE FOR LONGITUDE= 262.5
LAT + 5 ENERGIES WITH RMS ERROR + NO OF OBS + LINE TOTALS

-67.5	0.00	0.00	0.00	0.00	0.00	0.00	0.00	0.00	0.00	0.00	240	0.00	0.00
-37.5	0.00	0.00	0.00	0.00	0.00	0.00	0.00	0.00	0.00	0.00	348	0.00	0.00
-32.5	0.00	0.00	0.00	0.00	0.00	0.00	0.00	0.00	0.00	0.00	6720	0.00	0.00
-27.5	0.00	0.00	0.00	0.00	0.00	0.00	0.00	0.00	0.00	0.00	12312	0.00	0.00
-22.5	0.00	0.00	0.00	0.00	0.00	0.00	0.00	0.00	0.00	0.00	9132	0.00	0.00
-17.5	0.00	0.00	0.00	0.00	0.00	0.00	0.00	0.00	0.00	0.00	7512	0.00	0.00
-12.5	0.00	0.00	0.00	0.00	0.00	0.00	0.00	0.00	0.00	0.00	7116	0.00	0.00
-7.5	0.00	0.00	0.00	0.00	0.00	0.00	0.00	0.00	0.00	0.00	7464	0.00	0.00
-2.5	0.00	0.00	0.00	0.00	0.00	0.00	0.00	0.00	0.00	0.00	9552	0.00	0.00
2.5	0.00	0.00	0.00	0.00	0.00	0.00	0.00	0.00	0.00	0.00	[illegible]	0.00	0.00

OMNIDIRECTIONAL FLUX SUMMARY VS LATITUDE FOR LONGITUDE= 267.5
LAT + 5 ENERGIES WITH RMS ERROR + NO OF OBS + LINE TOTALS

-67.5	0.00	0.00	0.00	0.00	0.00	0.00	0.00	0.00	0.00	0.00	792	0.00	0.00
-42.5	0.00	0.00	0.00	0.00	0.00	0.00	0.00	0.00	0.00	0.00	1020	0.00	0.00
-37.5	0.00	0.00	0.00	0.00	0.00	0.00	0.00	0.00	0.00	0.00	5292	0.00	0.00
-32.5	0.00	0.00	0.00	0.00	0.00	0.00	0.00	0.00	0.00	0.00	9240	0.00	0.00
-27.5	.06	.06	0.00	0.00	0.00	0.00	0.00	0.00	0.00	0.00	9576	.03	.03
-22.5	0.00	0.00	.08	.08	.27	.19	.16	.16	.41	.41	11832	.10	.05
-17.5	.13	.07	.15	.10	0.00	0.00	0.00	0.00	.36	.36	13284	.11	.04
-12.5	.04	.04	0.00	0.00	.12	.12	0.00	0.00	.35	.35	13608	.05	.03
-7.5	0.00	0.00	.07	.07	0.00	0.00	0.00	0.00	0.00	0.00	13248	.02	.02
-2.5	0.00	0.00	0.00	0.00	0.00	0.00	0.00	0.00	0.00	0.00	12288	0.00	0.00
2.5	0.00	0.00	0.00	0.00	0.00	0.00	0.00	0.00	0.00	0.00	732	0.00	0.00

OMNIDIRECTIONAL FLUX SUMMARY VS LATITUDE FOR LONGITUDE= 272.5
LAT + 5 ENERGIES WITH RMS ERROR + NO OF OBS + LINE TOTALS

-67.5	0.00	0.00	0.00	0.00	0.00	0.00	0.00	0.00	0.00	0.00	1440	0.00	0.00
-47.5	0.00	0.00	0.00	0.00	0.00	0.00	0.00	0.00	0.00	0.00	1800	0.00	0.00
-42.5	0.00	0.00	.10	.10	0.00	0.00	0.00	0.00	0.00	0.00	9564	.03	.03
-37.5	.04	.04	0.00	0.00	0.00	0.00	0.00	0.00	0.00	0.00	13212	.02	.02
-32.5	.04	.04	0.00	0.00	.12	.12	.27	.19	0.00	0.00	13572	.07	.04
-27.5	.14	.08	.08	.08	0.00	0.00	0.00	0.00	.40	.40	11880	.10	.05
-22.5	.27	.12	.37	.18	.15	.15	.52	.30	0.00	0.00	10596	.29	.08
-17.5	.39	.16	.34	.20	.74	.37	.64	.37	0.00	0.00	8688	.44	.11
-12.5	.13	.10	.23	.17	.38	.27	0.00	0.00	0.00	0.00	8376	.17	.07
-7.5	0.00	0.00	0.00	0.00	0.00	0.00	0.00	0.00	0.00	0.00	8316	0.00	0.00
-2.5	0.00	0.00	0.00	0.00	0.00	0.00	0.00	0.00	0.00	0.00	8604	0.00	0.00
2.5	0.00	0.00	0.00	0.00	0.00	0.00	0.00	0.00	0.00	0.00	612	0.00	0.00

OMNIDIRECTIONAL FLUX SUMMARY VS LATITUDE FOR LONGITUDE= 277.5
LAT + 5 ENERGIES WITH RMS ERROR + NO OF OBS + LINE TOTALS

-67.5	0.00	0.00	0.00	0.00	0.00	0.00	0.00	0.00	0.00	0.00	3180	0.00	0.00
-52.5	0.00	0.00	0.00	0.00	0.00	0.00	0.00	0.00	0.00	0.00	1980	0.00	0.00
-47.5	0.00	0.00	0.00	0.00	0.00	0.00	0.00	0.00	0.00	0.00	10128	0.00	0.00
-42.5	.05	.05	0.00	0.00	0.00	0.00	.33	.24	0.00	0.00	11028	.07	.04
-37.5	.13	.09	0.00	0.00	.19	.19	0.00	0.00	0.00	0.00	8604	.08	.05
-32.5	.69	.24	.15	.15	.73	.42	0.00	0.00	0.00	0.00	6564	.44	.13
-27.5	.84	.24	.61	.27	1.40	.53	1.15	.51	1.79	1.04	8028	.96	.17
-22.5	1.91	.36	1.70	.39	2.32	.67	1.34	.55	2.90	1.30	8268	1.80	.23
-17.5	1.50	.30	.73	.28	1.02	.42	.95	.44	1.53	.88	9396	1.18	.17
-12.5	.59	.18	.37	.19	.45	.26	.88	.39	0.00	0.00	10475	.53	.11
-7.5	.16	.11	.13	.13	0.00	0.00	0.00	0.00	0.00	0.00	7284	.10	.06
-2.5	.09	.09	0.00	0.00	0.00	0.00	0.00	0.00	0.00	0.00	6516	.04	.04
2.5	0.00	0.00	0.00	0.00	0.00	0.00	0.00	0.00	0.00	0.00	[illegible]	0.00	0.00

OMNIDIRECTIONAL FLUX SUMMARY VS LATITUDE FOR LONGITUDE= 262.5

LAT + 5 ENERGIES WITH RMS ERROR + NO OF OBS + LINE TOTALS

-67.5	0.00	0.00	0.00	0.00	0.00	0.00	0.00	0.00	0.00	0.00	3864	0.00	0.00
-57.5	0.00	0.00	0.00	0.00	0.00	0.00	0.00	0.00	0.00	0.00	384	0.00	0.00
-52.5	0.00	0.00	0.00	0.00	0.00	0.00	0.00	0.00	0.00	0.00	6732	0.00	0.00
-47.5	0.00	0.00	0.00	0.00	0.00	0.00	0.00	0.00	0.00	0.00	6540	0.00	0.00
-42.5	.61	.23	.30	.21	.49	.35	1.42	.64	0.00	0.00	6492	.59	.15
-37.5	1.38	.32	.80	.73	2.39	.72	1.00	.50	2.60	1.30	7380	1.40	.21
-32.5	3.28	.46	4.24	.69	2.74	.71	2.95	.79	3.28	1.34	8772	3.39	.30
-27.5	3.28	.53	4.33	.66	2.69	.[illegible]1	3.66	1.02	.73	.73	6552	3.52	.36
-22.5	4.03	.55	5.83	.87	3.81	.90	5.86	1.20	6.98	2.11	7560	4.63	.39
-17.5	2.38	.43	2.75	.62	2.02	.67	3.63	.97	1.35	.95	7116	2.53	.29
-12.5	1.67	.38	.92	.37	.50	.35	2.62	.76	3.00	1.50	6408	1.42	.23
-7.5	.26	.13	.11	.11	.33	.27	.65	.37	0.00	0.00	8532	.28	.09
-2.5	0.00	0.00	0.00	0.00	0.00	0.00	0.00	0.00	0.00	0.00	8148	0.00	0.00
2.5	0.00	0.00	0.00	0.00	0.00	0.00	0.00	0.00	0.00	0.00	2064	0.00	0.00

OMNIDIRECTIONAL FLUX SUMMARY VS LATITUDE FOR LONGITUDE= 287.5

LAT + 5 ENERGIES WITH RMS ERROR + NO OF OBS + LINE TOTALS

-67.5	0.00	0.00	0.00	0.00	0.00	0.00	0.00	0.00	0.00	0.00	6208	0.00	0.00
-57.5	0.00	0.00	0.00	0.00	0.00	0.00	0.00	0.00	0.00	0.00	4404	0.00	0.00
-52.5	0.00	0.00	.12	.12	0.00	0.00	0.00	0.00	0.00	0.00	8496	.03	.03
-47.5	.34	.15	.71	.29	.19	.19	.22	.22	1.16	.82	8292	.43	.11
-42.5	1.69	.40	1.80	.54	2.93	.[illegible]6	3.38	1.62	4.80	1.36	6[illegible]00	2.28	.30
-37.5	5.35	.64	4.30	.76	5.71	1.12	7.10	1.34	7.25	2.19	7283	5.47	.42
-32.5	11.78	.94	10.81	1.19	11.48	1.56	12.[illegible]2	1.72	11.48	2.71	7524	11.52	.61
-27.5	8.32	.72	9.62	1.01	9.55	1.22	10.67	1.48	10.47	2.34	9168	9.11	.49
-22.5	7.99	.79	8.47	1.07	6.59	1.20	11.41	1.70	9.23	2.47	7284	8.40	.53
-17.5	5.43	.66	3.74	.72	4.75	1.[illegible]4	5.75	1.23	4.75	1.80	7068	4.92	.41
-12.5	1.66	.39	2.57	.64	4.98	1.14	2.42	.85	2.36	1.36	6111	2.51	.31
-7.5	.89	.26	.52	.25	.84	.42	.49	.34	1.26	.89	7593	.76	.15
-2.5	0.00	0.00	0.00	0.00	0.00	0.00	.24	.24	0.00	0.00	7775	.03	.03
2.5	0.00	0.00	0.00	0.00	0.00	0.00	0.00	0.00	0.00	0.00	4608	0.00	0.00

OMNIDIRECTIONAL FLUX SUMMARY VS LATITUDE FOR LONGITUDE= 292.5
LAT + 5 ENERGIES WITH RMS ERROR + NO OF OBS + LINE TOTALS

-67.5	0.00	0.00	0.00	0.00	0.00	0.00	0.00	0.00	0.00	0.00	11928	0.00	0.00
-62.5	0.00	0.00	0.00	0.00	0.00	0.00	0.00	0.00	0.00	0.00	5844	0.00	0.00
-57.5	0.00	0.00	0.00	0.00	0.00	0.00	0.00	0.00	0.00	0.00	8772	0.00	0.00
-52.5	.39	.15	.20	.14	.32	.23	.55	.32	0.00	0.00	10032	.33	.09
-47.5	1.60	.30	2.39	.48	2.50	.62	2.70	.70	3.75	1.32	10248	2.18	.23
-42.5	4.67	.53	5.71	.77	6.45	1.05	8.03	1.25	12.21	2.49	9432	6.01	.39
-37.5	12.74	.94	13.04	1.26	15.78	1.76	14.34	1.81	22.49	3.55	8112	13.97	.64
-32.5	22.69	1.42	21.06	1.80	21.65	2.34	24.92	2.69	24.11	4.26	6372	22.53	.92
-27.5	17.12	1.15	21.71	1.70	18.49	2.01	19.57	2.16	15.01	3.13	7355	18.53	.78
-22.5	14.42	.98	13.38	1.24	16.01	1.74	14.76	1.79	14.13	2.63	8496	14.44	.64
-17.5	9.41	.77	9.27	1.01	8.65	1.25	8.11	1.30	7.03	1.95	8880	8.97	.49
-12.5	5.16	.51	6.83	.78	5.21	.87	7.02	1.08	4.34	1.37	11049	5.78	.35
-7.5	.96	.23	1.11	.32	1.35	.45	2.09	.60	1.81	.91	10608	1.24	.17
-2.5	.11	.07	.18	.13	0.00	0.00	0.00	0.00	.45	.45	10716	.11	.05
2.5	0.00	0.00	0.00	0.00	0.00	0.00	0.00	0.00	0.00	0.00	7872	0.00	0.00

B10

OMNIDIRECTIONAL FLUX SUMMARY VS LATITUDE FOR LONGITUDE= 297.5
LAT + 5 ENERGIES WITH RMS ERROR + NO OF OBS + LINE TOTALS

-67.5	0.00	0.00	0.00	0.00	0.00	0.00	.29	.29	0.00	0.00	6456	.04	.04
-62.5	.06	.06	.10	.10	0.00	0.00	0.00	0.00	0.00	0.00	10069	.05	.03
-57.5	0.00	0.00	0.00	0.00	0.00	0.00	0.00	0.00	.44	.44	10800	.02	.02
-52.5	.46	.20	1.26	.45	1.55	.63	2.08	.79	2.32	1.34	6204	1.12	.21
-47.5	5.01	.68	4.74	.87	4.64	1.09	12.50	1.93	13.93	3.28	6203	6.31	.49
-42.5	12.12	.79	12.48	1.06	13.94	1.43	19.80	1.83	25.52	3.35	10908	14.15	.56
-37.5	22.83	1.00	22.63	1.32	26.97	1.33	34.72	2.24	33.34	3.53	12816	25.47	.69
-32.5	30.58	1.14	33.04	1.56	29.65	1.59	34.76	2.20	27.59	3.16	13224	31.44	.76
-27.5	31.25	1.22	32.08	1.63	30.87	2.04	33.74	2.30	29.65	3.47	11820	31.64	.80
-22.5	22.67	1.03	24.69	1.42	25.87	1.85	23.42	1.89	24.68	3.13	12060	23.84	.69
-17.5	14.46	.83	15.02	1.14	11.48	1.24	17.40	1.64	13.21	2.30	11983	14.72	.54
-12.5	8.60	.56	8.95	.75	9.23	.98	10.05	1.10	12.44	1.97	15432	9.16	.38
-7.5	2.89	.32	3.64	.48	4.20	.66	4.25	.71	3.38	1.02	15624	3.47	.23
-2.5	.24	.09	.24	.12	.39	.20	.34	.20	1.18	.59	16260	.32	.07
2.5	.07	.05	.06	.06	0.00	0.00	0.00	0.00	0.00	0.00	16080	.04	.03
7.5	0.00	0.00	0.00	0.00	0.00	0.00	0.00	0.00	0.00	0.00	2208	0.00	0.00

OMNIDIRECTIONAL FLUX SUMMARY VS LATITUDE FOR LONGITUDE= 302.5

LAT + 5 ENERGIES WITH RMS ERROR + NO OF OBS + LINE TOTALS

-67.5	0.00	0.00	0.00	0.00	0.00	0.00	0.00	0.00	.57	.57	8460	.03	.03
-62.5	.08	.08	0.00	0.00	0.00	0.00	0.00	0.00	.71	.71	6780	.07	.05
-57.5	.09	.09	.15	.15	.25	.25	.57	.41	.75	.75	6432	.22	.09
-52.5	2.04	.31	2.10	.41	2.90	.52	7.75	1.08	13.03	2.27	12156	3.48	.26
-47.5	5.91	.50	8.77	.51	10.55	1.13	28.00	1.98	42.95	3.35	13188	12.03	.47
-42.5	16.67	.96	18.19	1.33	23.66	1.94	43.57	2.82	65.41	5.57	10127	24.06	.76
-37.5	34.40	1.39	37.01	1.90	38.76	2.49	59.08	3.30	65.56	5.50	10032	40.46	.98
-32.5	43.59	1.27	47.27	1.74	44.94	2.17	49.19	2.44	59.08	4.31	15275	46.20	.85
-27.5	41.02	1.12	47.20	1.58	40.10	1.16	47.08	2.07	35.26	3.02	18516	42.38	.74
-22.5	31.18	.93	32.68	1.26	31.24	1.57	30.48	1.67	26.81	2.52	20232	31.25	.61
-17.5	20.23	.72	21.14	.97	21.13	1.25	22.56	1.38	21.33	2.17	21823	20.96	.48
-12.5	11.94	.63	9.90	.75	12.15	1.07	13.26	1.20	13.46	1.34	17124	11.72	.41
-7.5	5.17	.41	6.11	.59	4.85	.67	5.81	.78	4.40	1.10	17471	5.40	.27
-2.5	.60	.13	.63	.18	1.02	.30	.79	.28	.77	.44	18768	.70	.09
2.5	0.00	0.00	0.00	0.00	0.00	0.00	0.00	0.00	0.00	0.00	15036	0.00	0.00
7.5	0.00	0.00	0.00	0.00	0.00	0.00	0.00	0.00	0.00	0.00	5495	0.00	0.00

OMNIDIRECTIONAL FLUX SUMMARY VS LATITUDE FOR LONGITUDE= 307.5

LAT + 5 ENERGIES WITH RMS ERROR + NO OF OBS + LINE TOTALS

-67.5	0.00	0.00	0.00	0.00	0.00	0.00	0.00	0.00	.66	.56	7320	.03	.03
-62.5	.15	.11	.26	.18	0.00	0.00	.98	.49	.63	.63	7560	.29	.10
-57.5	.48	.17	.42	.21	1.37	.48	4.55	.95	9.77	2.24	9335	1.59	.20
-52.5	2.47	.38	4.19	.65	5.67	.57	19.26	1.93	42.06	4.59	9588	7.54	.43
-47.5	8.88	.59	13.38	.95	18.55	1.43	51.21	2.55	81.07	5.17	14567	20.55	.58
-42.5	19.76	.77	28.47	1.21	35.43	1.73	67.81	2.56	96.86	4.94	19032	34.35	.66
-37.5	39.46	1.00	44.71	1.40	49.28	1.57	76.03	2.50	92.85	4.46	22439	49.64	.73
-32.5	50.57	1.21	58.86	1.72	56.53	2.16	67.93	2.52	77.40	4.37	19475	56.98	.84
-27.5	47.91	1.18	50.25	1.59	50.23	2.34	57.77	2.35	52.30	3.50	19368	50.34	.79
-22.5	37.73	1.14	41.57	1.58	37.64	1.92	39.34	2.11	37.14	3.31	16284	38.84	.76
-17.5	26.57	1.07	30.23	1.50	28.07	1.54	32.25	2.12	17.79	2.54	13223	27.99	.71
-12.5	14.74	.74	15.35	.99	14.69	1.24	16.46	1.41	15.11	2.18	15251	15.12	.49
-7.5	6.87	.46	7.48	.66	5.50	.50	7.93	.93	7.16	1.43	16763	7.42	.33
-2.5	1.60	.23	1.95	.33	2.00	.43	1.89	.44	1.36	.61	17625	1.77	.16
2.5	.09	.05	.10	.07	0.00	0.00	.10	.10	.25	.25	19068	.09	.03
7.5	0.00	0.00	0.00	0.00	0.00	0.00	0.00	0.00	0.30	0.30	14520	0.00	0.00

OMNIDIRECTIONAL FLUX SUMMARY VS LATITUDE FOR LONGITUDE= 312.5

LAT + 5 ENERGIES WITH RMS ERROR + NO OF OBS + LINE TOTALS

-67.5	0.00	0.00	0.00	0.00	0.00	0.00	0.00	0.00	2.36	1.18	8148	.12	.06
-62.5	.11	.08	.10	.10	.96	.39	2.22	.64	5.76	1.66	9995	.79	.14
-57.5	.38	.12	1.80	.35	2.39	.51	10.54	1.15	29.37	3.10	14712	3.80	.25
-52.5	3.01	.29	4.57	.48	10.22	.91	34.25	1.79	82.25	4.47	19727	12.50	.39
-47.5	9.64	.57	13.77	.90	27.71	1.54	74.53	2.98	135.28	6.26	16572	28.08	.64
-42.5	23.83	.92	27.94	1.34	45.11	2.18	102.65	3.53	154.22	6.37	15252	44.46	.84
-37.5	42.23	1.35	46.67	1.87	59.83	2.71	95.29	3.67	130.66	6.93	13079	57.28	1.03
-32.5	56.30	1.51	62.47	2.10	66.45	2.77	90.76	3.47	86.03	5.45	13894	65.30	1.06
-27.5	56.70	1.47	59.45	1.98	57.17	2.48	63.31	2.93	59.64	4.38	14690	59.24	.98
-22.5	42.10	1.11	48.44	1.57	42.49	1.87	47.41	2.13	35.96	2.99	19355	44.10	.74
-17.5	31.29	.90	33.01	1.21	30.52	1.49	32.93	1.64	26.81	2.42	22020	31.47	.59
-12.5	16.93	.65	18.63	.90	17.40	1.12	16.77	1.18	16.76	1.90	22344	17.39	.43
-7.5	8.42	.49	9.12	.67	9.04	.86	8.92	.92	8.55	1.44	19655	8.76	.33
-2.5	2.10	.28	1.92	.35	1.88	.44	3.50	.65	2.20	.83	15286	2.25	.19
2.5	.44	.16	.19	.14	.31	.22	.18	.18	0.00	0.00	10234	.30	.06
7.5	0.00	0.00	0.00	0.00	0.00	0.00	0.00	0.00	0.00	0.00	9084	0.00	0.00

B12

OMNIDIRECTIONAL FLUX SUMMARY VS LATITUDE FOR LONGITUDE= 317.5

LAT + 5 ENERGIES WITH RMS ERROR + NO OF OBS + LINE TOTALS

-67.5	0.00	0.00	0.00	0.00	0.00	0.00	0.00	0.00	1.75	.88	10944	.09	.04
-62.5	.09	.05	.32	.13	.35	.17	4.73	.69	20.92	2.34	16360	1.83	.15
-57.5	.63	.14	.32	.21	4.08	.50	14.65	1.22	60.72	4.02	18024	6.02	.28
-52.5	3.21	.38	5.42	.64	12.21	1.23	44.29	2.52	129.73	6.96	12840	16.77	.56
-47.5	11.95	.77	15.36	1.14	35.67	2.23	105.43	4.14	219.87	9.59	11484	39.02	.90
-42.5	24.39	1.03	36.24	1.66	56.09	2.64	140.73	4.48	197.99	8.58	12923	55.85	1.02
-37.5	42.19	1.21	51.75	1.76	61.54	2.45	121.51	3.71	160.25	6.86	16356	63.70	.97
-32.5	58.17	1.40	67.09	1.98	78.50	2.73	105.94	3.41	110.63	5.62	16836	72.24	1.01
-27.5	60.08	1.51	67.67	2.11	64.75	2.63	77.18	3.09	72.68	4.33	14927	65.49	1.03
-22.5	48.98	1.44	50.88	1.94	47.47	2.39	56.02	2.79	48.92	4.21	13248	50.13	.95
-17.5	31.89	1.30	37.24	1.65	30.25	2.13	39.59	2.62	31.91	3.79	10680	33.96	.87
-12.5	18.51	1.00	22.62	1.45	20.22	1.75	24.21	2.06	18.25	2.88	10524	20.50	.68
-7.5	9.05	.69	9.00	.91	9.00	1.16	11.42	1.41	9.00	2.01	10668	9.34	.46
-2.5	2.68	.36	3.05	.51	2.63	.50	3.19	.71	4.56	1.37	11580	2.92	.25
2.5	.49	.15	.34	.17	0.00	0.00	.48	.28	0.00	0.00	11592	.35	.09
7.5	0.00	0.00	0.00	0.00	0.00	0.00	0.00	0.00	0.00	0.00	12936	0.00	0.00

OMNIDIRECTIONAL FLUX SUMMARY VS LATITUDE FOR LONGITUDE= 322.5
LAT + 5 ENERGIES WITH RMS ERROR + NO OF OBS + LINE TOTALS

-67.5	.03	.03	0.00	0.00	0.00	0.00	.31	.18	5.57	1.22	18084	.38	.07
-62.5	0.00	0.00	.12	.08	2.04	.45	7.75	.93	27.74	2.35	16440	2.73	.20
-57.5	.48	.14	1.65	.35	6.37	.88	31.54	2.11	130.01	6.06	13056	10.66	.44
-52.5	3.92	.38	6.61	.65	15.93	1.29	74.15	2.99	210.08	8.13	15264	25.82	.64
-47.5	9.85	.58	19.10	1.06	38.61	1.53	129.53	3.79	293.92	9.06	16620	45.69	.81
-42.5	21.85	.91	33.39	1.48	60.84	2.55	156.45	4.39	267.54	9.26	14964	60.31	.98
-37.5	36.54	1.36	45.38	1.99	67.27	3.10	138.42	4.78	200.94	9.28	11204	64.78	1.18
-32.5	54.29	1.74	61.47	2.44	65.10	3.20	120.03	4.67	134.29	7.97	10152	70.22	1.29
-27.5	59.66	1.83	77.54	2.75	70.73	3.76	83.46	3.92	91.29	6.51	10044	70.38	1.30
-22.5	49.72	1.76	59.57	2.54	54.51	3.11	57.57	3.43	51.67	5.25	9012	53.80	1.20
-17.5	35.03	1.58	32.09	1.99	31.13	2.50	42.54	3.14	33.74	4.51	7968	34.67	1.02
-12.5	19.19	1.40	21.25	1.94	18.51	2.31	27.03	3.00	26.03	4.75	5532	20.96	.95
-7.5	9.96	1.13	9.64	1.47	12.82	2.17	12.68	2.32	7.69	2.31	4368	10.55	.76
-2.5	2.25	.49	1.67	.56	3.94	1.09	4.20	1.21	4.55	2.03	5280	2.73	.35
2.5	.43	.19	.90	.37	.73	.42	1.41	.63	1.47	1.04	6552	.77	.17
7.5	0.00	0.00	.13	.13	0.00	0.00	0.00	0.00	0.00	0.00	7415	.03	.03

B13

OMNIDIRECTIONAL FLUX SUMMARY VS LATITUDE FOR LONGITUDE= 327.5
LAT + 5 ENERGIES WITH RMS ERROR + NO OF OBS + LINE TOTALS

-67.5	0.00	0.00	.05	.06	0.00	0.00	.24	.17	4.11	1.14	15180	.25	.06
-62.5	0.00	0.00	.14	.10	1.02	.34	6.44	.92	41.34	3.76	14052	3.09	.23
-57.5	.78	.11	1.79	.33	4.68	.58	40.94	2.15	146.21	6.54	16416	13.93	.45
-52.5	3.47	.38	6.95	.71	13.35	1.25	72.00	3.12	273.62	9.80	13667	28.22	.70
-47.5	10.62	.73	16.17	1.18	40.40	2.39	148.17	4.91	337.35	11.96	11327	50.67	1.04
-42.5	20.61	1.08	30.14	1.72	59.53	3.09	184.35	5.85	330.65	12.63	9945	65.57	1.26
-37.5	34.14	1.50	46.23	2.31	69.31	3.61	170.35	6.06	264.64	12.22	8519	71.62	1.42
-32.5	52.80	2.16	59.74	3.02	68.05	4.13	140.00	6.36	179.38	11.50	6396	74.45	1.67
-27.5	56.75	2.23	64.63	3.13	70.75	4.18	99.91	5.34	92.03	8.26	6468	68.17	1.59
-22.5	50.61	2.26	53.55	3.07	52.48	3.98	57.90	4.38	56.78	6.99	5580	52.86	1.51
-17.5	34.38	1.77	40.98	2.55	31.27	2.54	45.60	3.01	46.52	6.01	6192	37.99	1.21
-12.5	23.26	1.47	22.60	1.91	26.37	2.54	21.60	2.56	22.94	4.26	6063	23.33	.96
-7.5	8.72	.81	10.54	1.22	12.39	1.69	11.12	1.72	12.39	2.92	6972	9.91	.56
-2.5	3.46	.67	3.56	.89	3.63	1.15	6.71	1.68	6.54	2.57	4404	4.09	.47
2.5	.21	.15	.54	.31	.89	.51	1.02	.59	.89	.39	5424	.53	.15
7.5	0.00	0.00	.39	.27	.72	.32	0.00	0.00	0.00	0.00	5052	.14	.08

OMNIDIRECTIONAL FLUX SUMMARY VS LATTITUDE FOR LONGITUDE= 332.5

LAT + 5 ENERGIES WITH RMS ERROR + NO OF OBS + LINE TOTALS

-67.5	0.00	0.00	0.00	0.00	.19	.14	.22	.16	2.03	.77	16536	.16	.05
-62.5	0.00	0.00	.07	.07	.64	.26	3.01	.68	30.67	3.13	15024	2.14	.18
-57.5	.16	.10	1.71	.40	5.59	.33	38.20	2.62	144.07	8.20	10296	13.50	.56
-52.5	2.45	.40	5.63	.79	15.00	1.66	93.92	4.45	352.29	13.90	3748	34.49	.97
-47.5	7.62	.81	13.56	1.41	35.85	2.94	166.63	5.80	433.25	17.59	6648	55.35	1.41
-42.5	15.63	1.18	27.58	2.07	65.15	4.07	205.54	7.77	422.17	17.95	6288	71.00	1.65
-37.5	29.49	1.57	41.47	2.45	67.26	3.98	186.26	7.12	279.67	14.07	6780	70.98	1.59
-32.5	42.67	2.00	49.18	2.83	69.99	4.31	146.21	6.69	180.53	11.98	6036	68.71	1.65
-27.5	50.53	2.27	60.73	3.28	64.65	4.32	108.57	6.01	129.01	10.57	5544	66.63	1.70
-22.5	49.58	2.63	58.38	3.51	53.67	4.60	51.47	5.29	56.82	8.20	4055	52.44	1.76
-17.5	31.82	2.05	37.49	2.94	36.06	3.58	36.84	4.00	34.93	6.27	4260	34.65	1.40
-12.5	20.69	1.50	17.85	1.84	20.16	2.50	24.33	2.95	17.68	4.06	5160	20.23	.97
-7.5	8.43	.93	9.80	1.32	9.61	1.57	10.75	1.90	9.61	2.30	5496	9.30	.64
-2.5	3.26	.58	4.06	.85	4.33	1.12	4.00	1.15	0.00	0.00	5544	3.55	.39
2.5	.20	.14	1.20	.45	1.63	.59	.65	.46	0.00	0.00	5795	.72	.17
7.5	0.00	0.00	0.00	0.00	0.00	0.00	0.00	0.00	0.00	0.00	7212	0.00	0.00

B/4

OMNIDIRECTIONAL FLUX SUMMARY VS LATTITUDE FOR LONGITUDE= 337.5

LAT + 5 ENERGIES WITH RMS ERROR + NO OF OBS + LINE TOTALS

-67.5	0.00	0.00	0.00	0.00	0.00	0.00	0.00	0.00	.61	.43	15612	.03	.02
-62.5	.05	.05	0.00	0.00	0.00	0.00	2.55	.64	19.36	2.37	11604	1.34	.17
-57.5	.16	.11	1.41	.45	6.22	1.00	32.95	2.96	176.87	11.05	6948	14.47	.71
-52.5	1.55	.41	3.64	.64	15.65	2.21	92.32	5.79	385.01	19.01	5112	35.21	1.29
-47.5	5.66	.79	11.36	1.48	30.51	3.10	142.25	7.18	476.45	21.20	5088	52.08	1.57
-42.5	15.69	1.36	28.84	2.42	58.05	4.39	212.80	9.02	461.73	21.44	4824	73.19	1.91
-37.5	22.32	1.73	35.92	2.09	65.53	5.00	203.53	9.46	324.60	19.26	4200	70.81	2.01
-32.5	33.89	1.91	45.50	2.92	62.08	4.36	141.51	7.07	234.86	14.59	5232	65.01	1.73
-27.5	44.61	2.18	52.20	3.11	60.47	4.28	112.34	6.26	110.67	10.02	5292	60.96	1.66
-22.5	44.45	2.20	53.17	3.17	57.28	4.20	65.03	4.81	68.37	7.95	5196	52.38	1.56
-17.5	32.97	1.77	35.37	2.42	27.81	2.74	34.56	3.28	40.50	5.73	5927	33.37	1.16
-12.5	20.40	1.26	15.60	1.45	16.61	1.92	23.00	2.42	20.60	3.70	7224	19.00	.79
-7.5	8.64	.74	7.71	.92	9.72	1.72	7.27	1.23	8.10	2.09	8692	8.37	.48
-2.5	2.23	.36	1.93	.44	2.16	.60	2.88	.74	2.49	1.12	9624	2.24	.24
2.5	.49	.16	.58	.24	.55	.28	.32	.23	0.00	0.00	11460	.50	.10
7.5	0.00	0.00	.10	.10	.33	.24	.39	.27	0.00	0.00	9564	.13	.06

OMNIDIRECTIONAL FLUX SUMMARY VS LATITUDE FOR LONGITUDE= 342.5

LAT + 5 ENERGIES WITH RMS ERROR + NO OF OBS + LINE TOTALS

-67.5	0.00	0.00	0.00	0.00	0.00	0.00	.21	.21	.55	.55	8772	.05	.04
-62.5	.09	.09	0.00	0.00	0.00	0.00	3.31	1.00	16.44	3.59	6132	1.29	.22
-57.5	0.00	0.00	.58	.26	3.42	.31	21.07	2.15	127.83	8.54	8412	9.79	.53
-52.5	1.52	.39	3.88	.83	13.25	1.95	95.06	5.62	381.09	18.15	5555	35.00	1.23
-47.5	4.86	.72	8.05	1.23	28.44	[illegible]	152.45	7.33	559.68	22.66	5232	56.11	1.60
-42.5	10.57	1.06	19.61	1.91	45.96	[illegible]	210.03	6.56	571.48	22.77	5292	72.11	1.81
-37.5	19.23	1.40	33.19	2.41	71.12	4.52	216.39	8.46	448.21	19.64	5580	77.51	1.83
-32.5	26.02	1.41	39.82	2.30	65.55	3.80	160.11	5.33	264.74	13.12	7380	64.85	1.45
-27.5	33.85	1.44	44.46	2.17	54.51	[illegible]	107.66	4.63	145.34	8.59	9275	54.75	1.19
-22.5	35.68	1.40	39.78	1.94	42.33	2.56	59.75	3.27	71.63	5.77	10320	42.61	1.00
-17.5	26.86	1.23	30.68	1.73	25.34	[illegible]	36.96	2.60	40.31	4.41	10092	29.66	.84
-12.5	15.93	1.12	15.52	1.45	18.45	2.03	15.39	1.99	18.01	3.47	7198	16.24	.74
-7.5	6.28	.82	7.32	1.17	7.05	1.47	8.84	1.77	3.68	1.84	5220	6.85	.56
-2.5	2.09	.60	2.72	.91	3.45	1.71	3.99	1.51	1.48	1.48	3239	2.67	.44
2.5	.61	.35	1.76	.79	0.00	0.00	.66	.66	0.00	0.00	2784	.78	.26
7.5	.23	.23	0.00	0.00	0.00	0.00	0.00	0.00	0.00	0.00	2424	.10	.10

OMNIDIRECTIONAL FLUX SUMMARY VS LATITUDE FOR LONGITUDE= 347.5

LAT + 5 ENERGIES WITH RMS ERROR + NO OF OBS + LINE TOTALS

-67.5	0.00	0.00	0.00	0.00	0.00	0.00	0.00	0.00	0.00	0.00	5376	0.00	0.00
-62.5	0.00	0.00	0.00	0.00	0.00	0.00	.40	.40	4.12	2.06	4656	.26	.12
-57.5	0.00	0.00	.24	.24	.78	.55	15.60	2.73	103.80	11.00	4115	7.52	.66
-52.5	.63	.28	4.31	.63	14.58	[illegible]	94.56	5.34	385.97	17.37	6144	35.24	1.17
-47.5	3.32	.44	10.80	1.05	23.34	1.98	154.63	5.47	591.48	17.26	9528	57.23	1.20
-42.5	9.06	.65	18.51	1.22	45.62	2.44	201.38	5.50	614.71	15.30	12276	72.15	1.19
-37.5	16.62	.93	29.54	1.63	54.10	[illegible]	229.46	6.22	493.07	14.71	10943	76.90	1.30
-32.5	25.29	1.46	38.79	2.37	54.81	3.61	171.65	6.86	320.31	15.10	6744	66.80	1.54
-27.5	26.29	1.87	36.43	2.79	48.65	4.13	107.82	6.60	155.39	12.77	4572	53.03	1.62
-22.5	30.24	2.39	33.44	3.31	43.38	4.82	60.55	6.12	83.54	11.59	2988	39.60	1.78
-17.5	29.86	3.89	21.07	4.30	31.54	6.73	31.43	7.21	47.32	14.27	1116	29.03	2.50
-12.5	11.15	2.15	9.31	2.58	11.70	3.70	14.85	4.48	10.53	6.08	1368	11.23	1.40
-7.5	4.24	1.34	1.47	1.04	3.60	[illegible]	2.77	1.96	0.00	0.00	1332	3.06	.74
-2.5	1.68	.71	2.33	1.04	1.52	[illegible]	1.76	1.24	2.29	2.29	2100	1.94	.47
2.5	.22	.22	.76	.54	0.00	0.00	.72	.72	0.00	0.00	2563	.37	.19
7.5	.12	.12	0.00	0.00	0.00	0.00	0.00	0.00	0.00	0.00	4764	.05	.05

B16

OMNIDIRECTIONAL FLUX SUMMARY VS LATITUDE FOR LONGITUDE= 352.5

LAT + 5 ENERGIES WITH RMS ERROR + NO OF OBS + LINE TOTALS

-67.5	0.00	0.00	0.00	0.00	.44	.44	0.00	0.00	0.00	0.00	3599	.07	.07
-62.5	0.00	0.00	0.00	0.00	0.00	0.00	0.00	0.00	4.28	1.92	5604	.21	.10
-57.5	0.00	0.00	.38	.22	.61	.35	8.97	1.45	55.83	5.85	7824	4.14	.36
-52.5	.41	.16	2.46	.50	11.70	1.40	66.06	3.62	333.86	12.94	9575	28.07	.84
-47.5	2.03	.44	8.20	1.17	27.95	2.72	158.90	7.08	590.21	22.30	5856	57.09	1.53
-42.5	6.45	1.02	12.30	1.85	37.90	4.16	184.35	9.97	613.75	29.00	3504	66.17	2.13
-37.5	15.15	1.65	29.09	3.02	55.69	5.33	213.99	11.23	505.79	27.34	3132	75.03	2.40
-32.5	19.45	1.78	29.76	2.90	54.63	5.73	166.28	9.48	341.69	21.79	3456	62.71	2.09
-27.5	21.20	1.85	30.37	2.91	47.33	4.64	95.10	7.10	147.45	14.19	3516	43.42	1.72
-22.5	22.29	1.81	25.43	2.54	29.91	3.52	40.74	4.42	51.09	7.96	3652	28.04	1.32
-17.5	17.47	1.76	19.79	2.47	16.67	2.90	23.89	3.73	34.85	7.27	3168	19.62	1.22
-12.5	8.56	1.16	7.15	1.40	5.74	1.74	9.85	2.26	12.13	4.04	3563	8.29	.75
-7.5	1.76	.59	1.02	.59	.55	.55	3.83	1.56	3.32	2.35	2892	1.74	.38
-2.5	.36	.21	.21	.21	.69	.49	0.00	0.00	1.03	1.03	4642	.36	.14
2.5	.10	.10	0.00	0.00	0.00	0.00	0.00	0.00	0.00	0.00	5532	.04	.04
7.5	0.00	0.00	0.00	0.00	.35	.35	.40	.40	0.00	0.00	4572	.10	.07

OMNIDIRECTIONAL FLUX SUMMARY VS LATITUDE FOR LONGITUDE= 357.5

LAT + 5 ENERGIES WITH RMS ERROR + NO OF OBS + LINE TOTALS

-67.5	0.00	0.00	0.00	0.00	0.00	0.00	0.00	0.00	0.00	0.00	2412	0.00	0.00
-62.5	.32	.12	0.00	0.00	0.00	0.00	0.00	0.00	2.75	1.04	12239	.27	.07
-57.5	0.00	0.00	0.00	0.00	0.00	0.00	3.00	.80	44.51	4.98	8628	2.61	.27
-52.5	.19	.19	1.61	.72	6.30	1.52	46.04	5.28	277.19	20.69	3048	21.26	1.29
-47.5	2.08	.93	4.33	1.77	23.60	5.28	166.11	15.04	715.10	50.31	1356	62.84	3.34
-42.5	1.72	.99	8.96	2.99	32.52	7.27	153.86	16.99	731.77	59.75	984	64.40	3.96
-37.5	11.44	1.93	27.21	3.93	42.60	6.28	230.79	15.70	600.05	40.93	1728	77.92	3.29
-32.5	13.14	1.70	29.63	3.35	60.80	6.14	168.95	11.00	348.07	25.45	2579	61.33	2.39
-27.5	19.63	2.09	21.28	2.87	33.49	4.60	102.09	3.63	121.34	15.17	2532	37.92	1.90
-22.5	18.25	1.37	20.10	1.89	22.65	2.57	46.93	3.97	50.55	6.64	5508	24.71	1.04
-17.5	10.55	.98	12.76	1.39	13.79	1.65	13.56	2.00	14.56	3.34	6264	12.07	.68
-12.5	4.92	.72	2.72	.70	4.15	1.11	3.76	1.13	8.99	2.57	5400	4.27	.44
-7.5	.82	.27	.32	.22	.51	.76	.59	.51	3.09	1.54	6215	.77	.17
-2.5	.26	.18	0.00	0.00	0.00	0.00	0.00	0.00	0.00	0.00	4344	.11	.08
2.5	0.00	0.00	0.00	0.00	0.00	0.00	0.00	0.00	0.00	0.00	3957	0.00	0.00
7.5	0.00	0.00	0.00	0.00	0.00	0.00	0.00	0.00	0.00	0.00	5592	0.00	0.00

OMNIDIRECTIONAL FLUX SUMMARY VS LATITUDE FOR LONGITUDE= 2.5

LAT + 5 ENERGIES WITH RMS ERROR + NO OF OBS + LINE TOTALS

-67.5	0.00	0.00	0.00	0.00	0.00	0.00	0.00	0.00	0.00	0.00	672	0.00	0.00
-62.5	0.00	0.00	0.00	0.00	0.00	0.00	.40	.40	2.08	1.47	4608	.16	.09
-57.5	0.00	0.00	0.00	0.00	0.00	0.00	1.71	.86	22.29	4.98	4308	1.34	.27
-52.5	0.00	0.00	.41	.29	3.04	1.01	26.68	3.24	196.47	14.11	4743	13.67	.84
-47.5	.96	.34	3.32	.52	17.98	2.47	119.41	6.84	539.48	23.43	4716	46.42	1.54
-42.5	2.93	.55	8.76	1.23	26.13	2.79	154.29	8.16	739.48	25.67	5386	63.45	1.76
-37.5	5.73	.84	16.71	1.85	38.69	3.66	185.75	8.60	610.41	25.15	4632	67.00	1.86
-32.5	12.52	1.45	21.14	2.47	50.61	4.89	149.54	9.03	300.82	20.66	3383	52.57	1.93
-27.5	13.58	1.45	21.41	2.79	35.85	7.06	78.69	6.30	152.14	14.13	3660	34.23	1.50
-22.5	11.27	2.45	14.84	3.71	13.64	4.55	17.99	4.95	36.37	12.86	1056	14.09	1.79
-17.5	8.11	2.10	10.32	7.11	6.13	3.77	7.97	3.54	0.00	0.00	1044	7.82	1.34
-12.5	.60	.60	3.10	1.79	0.00	0.00	0.00	0.00	5.06	5.06	948	1.27	.57
-7.5	.65	.65	1.13	1.13	1.85	1.85	2.14	2.14	0.00	0.00	664	1.11	.56
-2.5	0.00	0.00	0.00	0.00	0.00	0.00	1.12	1.12	0.00	0.00	1652	.15	.15
2.5	0.00	0.00	0.00	0.00	0.00	0.00	0.00	0.00	0.00	0.00	3804	0.00	0.00
7.5	0.00	0.00	0.00	0.00	0.00	0.00	0.00	0.00	0.00	0.00	4775	0.00	0.00

817

OMNIDIRECTIONAL FLUX SUMMARY VS LATITUDE FOR LONGITUDE= 7.5

LAT + 5 ENERGIES WITH RMS ERROR + NO OF OBS + LINE TOTALS

-62.5	0.00	0.00	0.00	0.00	0.00	0.00	0.00	0.00	0.00	0.00	5796	0.00	0.00
-57.5	.17	.17	0.00	0.00	0.00	0.00	.57	.57	8.59	3.53	3240	.59	.21
-52.5	.09	.09	.45	.28	1.30	.58	15.03	2.12	114.85	9.47	6144	8.05	.56
-47.5	.50	.20	2.59	.61	13.62	1.79	78.55	4.61	433.13	17.47	6816	34.76	1.11
-42.5	2.34	.48	6.42	1.04	16.01	2.10	163.10	7.21	690.74	23.92	5796	60.71	1.59
-37.5	5.73	.89	14.05	1.84	32.05	3.56	144.27	8.12	517.55	24.79	4044	55.32	1.81
-32.5	8.39	1.26	19.52	2.47	31.86	4.15	160.76	10.01	346.32	23.76	2963	51.20	2.04
-27.5	10.24	1.42	13.32	2.43	27.34	3.01	79.83	7.17	130.55	14.75	2868	28.62	1.55
-22.5	7.70	1.51	6.77	2.12	8.39	2.65	21.29	4.54	35.22	9.41	1908	11.20	1.19
-17.5	5.88	1.77	0.00	0.00	7.58	3.39	3.50	2.47	0.00	0.00	1056	4.09	.96
-12.5	1.34	.78	1.56	1.10	1.27	1.27	1.47	1.47	0.00	0.00	1260	1.33	.50
-7.5	0.00	0.00	0.00	0.00	0.00	0.00	0.00	0.00	0.00	0.00	1224	0.00	0.00
-2.5	0.00	0.00	0.00	0.00	0.00	0.00	0.00	0.00	0.00	0.00	1044	0.00	0.00
2.5	0.00	0.00	0.00	0.00	0.00	0.00	0.00	0.00	0.00	0.00	3108	0.00	0.00
7.5	0.00	0.00	0.00	0.00	0.00	0.00	0.00	0.00	0.00	0.00	5985	0.00	0.00

OMNIDIRECTIONAL FLUX SUMMARY VS LATITUDE FOR LONGITUDE= 12.5
LAT + 5 ENERGIES WITH RMS ERROR + NO OF OBS + LINE TOTALS

-62.5	0.00	0.00	0.00	0.00	0.00	0.00	.30	.30	0.00	0.00	6132	.04	.04
-57.5	0.00	0.00	0.00	0.00	.13	.13	.15	.15	3.17	1.12	12095	.20	.06
-52.5	0.00	0.00	0.00	0.00	.25	.26	4.54	1.17	41.74	5.73	6096	2.72	.33
-47.5	0.00	0.00	2.04	1.18	2.22	1.57	34.62	6.66	180.01	24.50	1440	14.33	1.55
-42.5	2.35	.96	5.44	1.92	11.11	3.51	123.09	12.56	553.38	42.95	1449	47.67	2.82
-37.5	4.53	.91	12.56	1.99	29.75	3.21	161.55	9.78	543.12	28.91	3120	57.62	2.11
-32.5	9.99	1.12	16.89	1.91	31.83	3.36	131.41	7.32	281.19	17.27	4524	44.30	1.53
-27.5	9.89	1.14	11.89	1.65	19.80	2.72	54.73	4.66	98.61	10.51	4284	22.13	1.11
-22.5	6.15	.86	6.07	1.13	8.89	1.74	12.23	2.20	21.54	4.70	4680	8.10	.64
-17.5	2.26	.41	2.75	.63	1.71	.60	2.96	.65	3.85	1.57	7487	2.47	.28
-12.5	.06	.06	.33	.19	.18	.18	0.00	0.00	0.00	0.00	8987	.13	.06
-7.5	.06	.06	.21	.15	0.00	0.00	0.00	0.00	.51	.51	9348	.10	.05
-2.5	.06	.06	.10	.10	0.00	0.00	0.00	0.00	0.00	0.00	10176	.05	.03
2.5	0.00	0.00	0.00	0.00	0.00	0.00	0.00	0.00	0.00	0.00	7104	0.00	0.00
7.5	0.00	0.00	0.00	0.00	0.00	0.00	0.00	0.00	0.00	0.00	5544	0.00	0.00

818

OMNIDIRECTIONAL FLUX SUMMARY VS LATITUDE FOR LONGITUDE= 17.5
LAT + 5 ENERGIES WITH RMS ERROR + NO OF OBS + LINE TOTALS

-62.5	0.00	0.00	0.00	0.00	0.00	0.00	0.00	0.00	0.00	0.00	3300	0.00	0.00
-57.5	.05	.05	.08	.08	.13	.13	0.00	0.00	.79	.56	12204	.10	.04
-52.5	0.00	0.00	.11	.11	0.00	0.00	1.79	.60	27.46	3.77	9264	1.63	.21
-47.5	.13	.09	.91	.32	3.52	.81	26.93	2.40	193.37	10.37	8639	13.97	.62
-42.5	.06	.28	4.87	.66	17.66	2.10	106.50	5.58	514.22	19.59	6432	44.03	1.28
-37.5	4.60	.60	8.93	1.11	21.33	2.19	122.79	5.64	495.73	18.27	7127	43.09	1.27
-32.5	7.12	.74	14.51	1.40	22.60	2.23	105.05	5.16	287.60	13.76	7294	38.01	1.12
-27.5	6.71	.73	11.78	1.27	16.33	1.91	47.25	3.49	94.65	7.97	7151	19.06	.80
-22.5	4.58	.54	6.94	.89	6.04	1.35	11.19	1.54	13.72	2.74	8747	6.70	.43
-17.5	1.05	.27	1.45	.42	.99	.44	.68	.40	2.97	1.33	8089	1.19	.19
-12.5	.07	.07	.12	.12	0.00	0.00	.44	.31	0.00	0.00	8484	.11	.06
-7.5	0.00	0.00	0.00	0.00	0.00	0.00	0.00	0.00	0.00	0.00	7968	0.00	0.00
-2.5	0.00	0.00	0.00	0.00	0.00	0.00	0.00	0.00	0.00	0.00	8700	0.00	0.00
2.5	0.00	0.00	0.00	0.00	0.00	0.00	0.00	0.00	0.00	0.00	10296	0.00	0.00
7.5	0.00	0.00	0.00	0.00	0.00	0.00	0.00	0.00	0.00	0.00	8664	0.00	0.00

OMNIDIRECTIONAL FLUX SUMMARY VS LATITUDE FOR LONGITUDE= 22.5
LAT + 5 ENERGIES WITH RMS ERROR + NO OF OBS + LINE TOTALS

-62.5	0.00	0.00	0.00	0.00	0.00	0.00	0.00	0.00	0.00	0.00	168	0.00	0.00
-57.5	.06	.06	0.00	0.00	0.00	0.00	0.00	0.00	3.11	1.27	9252	.18	.07
-52.5	0.00	0.00	0.00	0.00	0.00	0.00	1.07	.38	22.65	2.81	13776	1.27	.15
-47.5	.03	.03	.25	.11	2.20	.42	16.27	1.24	144.76	5.05	19631	9.76	.35
-42.5	.50	.13	3.22	.43	14.38	1.16	83.93	3.02	379.76	10.35	17027	33.06	.68
-37.5	2.56	.32	7.34	.72	15.91	1.35	124.68	4.08	448.12	12.45	13883	43.91	.87
-32.5	5.42	.47	10.17	.84	24.52	1.68	85.39	3.36	238.51	9.05	13968	31.50	.74
-27.5	4.85	.47	7.94	.79	15.70	1.43	75.47	2.30	68.10	5.15	12335	14.38	.53
-22.5	1.70	.70	2.67	.50	3.01	.67	6.25	1.04	8.13	1.32	10631	3.05	.26
-17.5	.71	.20	.51	.23	.50	.29	0.00	0.00	0.00	0.00	9552	.50	.11
-12.5	0.00	0.00	0.00	0.00	0.00	0.00	0.00	0.00	0.00	0.00	5688	0.00	0.00
-7.5	0.00	0.00	0.00	0.00	0.00	0.00	0.00	0.00	0.00	0.00	6755	0.00	0.00
-2.5	0.00	0.00	0.00	0.00	0.00	0.00	0.00	0.00	0.00	0.00	6144	0.00	0.00
2.5	0.00	0.00	0.00	0.00	0.00	0.00	0.00	0.00	0.00	0.00	7128	0.00	0.00
7.5	0.00	0.00	0.00	0.00	0.00	0.00	0.00	0.00	0.00	0.00	7920	0.00	0.00

B19

OMNIDIRECTIONAL FLUX SUMMARY VS LATITUDE FOR LONGITUDE= 27.5
LAT + 5 ENERGIES WITH RMS ERROR + NO OF OBS + LINE TOTALS

-57.5	.05	.05	0.00	0.00	0.00	0.00	0.00	0.00	.39	.39	12252	.04	.03
-52.5	.06	.04	0.00	0.00	0.00	0.00	.62	.29	8.31	1.49	17904	.55	.09
-47.5	0.00	0.00	.29	.11	1.17	.35	12.06	1.22	87.05	5.28	15000	6.14	.31
-42.5	.39	.12	2.05	.36	11.18	1.17	66.14	2.79	318.01	9.05	15744	26.85	.64
-37.5	1.81	.23	5.87	.55	18.91	1.27	99.45	3.13	369.73	9.74	18696	36.46	.68
-32.5	4.49	.39	9.66	.75	16.07	1.24	66.33	2.71	200.88	7.59	16728	25.35	.60
-27.5	5.27	.43	6.99	.64	9.61	.57	26.44	1.78	60.27	4.19	16488	12.08	.42
-22.5	1.83	.29	2.56	.44	2.91	.61	2.92	.65	3.42	1.14	12648	2.39	.21
-17.5	.10	.07	.33	.17	.82	.33	.63	.31	1.22	.71	11772	.39	.09
-12.5	0.00	0.00	0.00	0.00	0.00	0.00	0.00	0.00	0.00	0.00	12420	0.00	0.00
-7.5	0.00	0.00	0.00	0.00	0.00	0.00	0.00	0.00	0.00	0.00	11388	0.00	0.00
-2.5	0.00	0.00	0.00	0.00	0.00	0.00	0.00	0.00	0.00	0.00	10824	0.00	0.00
2.5	0.00	0.00	0.00	0.00	0.00	0.00	0.00	0.00	0.00	0.00	9612	0.00	0.00
7.5	0.00	0.00	0.00	0.00	0.00	0.00	0.00	0.00	0.00	0.00	6204	0.00	0.00

OMNIDIRECTIONAL FLUX SUMMARY VS LATITUDE FOR LONGITUDE= 32.5

LAT + 5 ENERGIES WITH RMS ERROR + NO OF OBS + LINE TOTALS

-57.5	0.00	0.00	0.00	0.00	0.00	0.00	.27	.27	5.66	2.10	6780	.32	.11
-52.5	0.00	0.00	.22	.11	0.00	0.00	.21	.15	1.93	.73	17448	.18	.05
-47.5	0.00	0.00	.06	.06	.30	.17	5.71	.82	54.81	4.07	15852	3.54	.23
-42.5	.34	.11	1.60	.31	6.58	[illegible]	[illegible]	2.12	196.25	7.55	16535	16.55	.49
-37.5	1.45	.24	3.74	.50	9.78	1.04	76.68	3.14	271.71	9.52	14393	26.55	.67
-32.5	3.04	.35	5.96	.64	11.52	1.14	49.05	2.52	133.24	6.59	14303	17.52	.54
-27.5	3.60	.39	4.75	.59	6.43	[illegible]	16.94	1.54	27.66	3.17	13188	7.24	.36
-22.5	1.03	.19	2.09	.35	1.56	.39	2.58	.54	2.63	.88	16439	1.65	.16
-17.5	.10	.06	0.00	0.00	.10	.10	.11	.11	0.00	0.00	16164	.07	.03
-12.5	0.00	0.00	0.00	0.00	.28	.16	0.00	0.00	0.00	0.00	17388	.04	.02
-7.5	0.00	0.00	0.00	0.00	0.00	0.00	0.00	0.00	0.00	0.00	8844	0.00	0.00
-2.5	0.00	0.00	0.00	0.00	0.00	0.00	0.00	0.00	0.00	0.00	7856	0.00	0.00
2.5	0.00	0.00	0.00	0.00	0.00	0.00	0.00	0.00	0.00	0.00	10812	0.00	0.00
7.5	0.00	0.00	0.00	0.00	0.00	0.00	0.00	0.00	0.00	0.00	1764	0.00	0.00

820

OMNIDIRECTIONAL FLUX SUMMARY VS LATITUDE FOR LONGITUDE= 37.5

LAT + 5 ENERGIES WITH RMS ERROR + NO OF OBS + LINE TOTALS

-57.5	0.00	0.00	0.00	0.00	0.00	0.00	0.00	0.00	0.00	0.00	3060	0.00	0.00
-52.5	0.00	0.00	0.00	0.00	0.00	0.00	0.00	0.00	1.10	.55	17448	.06	.03
-47.5	0.00	0.00	0.00	0.00	.09	[illegible]	2.76	.54	26.23	2.59	17388	1.68	.15
-42.5	.16	.07	.40	.15	4.62	.65	24.75	1.63	116.51	5.69	17304	9.98	.37
-37.5	.70	.15	2.80	.39	8.07	.35	43.63	2.12	158.62	6.53	17856	15.79	.46
-32.5	1.81	.23	4.12	.46	7.25	.79	22.53	1.49	65.99	4.11	18768	9.09	.34
-27.5	1.61	.22	2.31	.35	3.34	.54	5.88	.77	9.76	1.50	18204	3.01	.20
-22.5	.68	.15	.50	.17	1.01	.30	.64	.30	.55	.39	17508	.70	.10
-17.5	0.00	0.00	.05	.06	0.00	0.00	0.00	0.00	0.00	0.00	15624	.02	.02
-12.5	0.00	0.00	0.00	0.00	0.00	0.00	0.00	0.00	0.00	0.00	12312	0.00	0.00
-7.5	0.00	0.00	0.00	0.00	0.00	0.00	0.00	0.00	0.00	0.00	504	0.00	0.00
-2.5	0.00	0.00	0.00	0.00	0.00	0.00	0.00	0.00	0.00	0.00	852	0.00	0.00
2.5	0.00	0.00	0.00	0.00	0.00	0.00	0.00	0.00	0.00	0.00	2100	0.00	0.00

OMNIDIRECTIONAL FLUX SUMMARY VS LATITUDE FOR LONGITUDE= 42.5
LAT + 5 ENERGIES WITH RMS ERROR + NO OF OBS + LINE TOTALS

-57.5	0.00	0.00	0.00	0.00	0.00	0.00	0.00	0.00	0.00	0.00	36	0.00	0.00
-52.5	0.00	0.00	0.00	0.00	.19	.14	0.00	0.00	.58	.41	16476	.06	.08
-47.5	0.00	0.00	0.00	0.00	.17	.12	1.45	.37	12.05	1.74	19123	.82	.10
-42.5	.03	.03	.53	.17	2.42	.46	17.29	1.15	72.21	4.33	18480	5.84	.28
-37.5	.40	.11	1.24	.25	3.32	.52	20.02	1.37	63.23	3.92	19740	6.74	.29
-32.5	.91	.16	1.72	.29	3.05	.49	5.38	.77	17.31	2.04	19969	2.96	.19
-27.5	.52	.12	.52	.16	1.09	.29	1.80	.40	1.64	.52	20544	.83	.10
-22.5	.28	.09	.19	.10	.16	.11	.18	.13	0.00	0.00	20232	.21	.05
-17.5	0.00	0.00	0.00	0.00	0.00	0.00	0.00	0.00	0.00	0.00	19704	0.00	0.00
-12.5	0.00	0.00	0.00	0.00	0.00	0.00	0.00	0.00	0.00	0.00	4032	0.00	0.00

OMNIDIRECTIONAL FLUX SUMMARY VS LATITUDE FOR LONGITUDE= 47.5
LAT + 5 ENERGIES WITH RMS ERROR + NO OF OBS + LINE TOTALS

-52.5	0.00	0.00	.15	.10	0.00	0.00	0.00	0.00	0.00	0.00	13416	.04	.03
-47.5	0.00	0.00	0.00	0.00	0.00	0.00	.57	.23	7.67	1.38	19392	.46	.08
-42.5	.06	.04	0.00	0.00	1.12	.70	5.27	.70	26.19	2.51	19980	2.19	.16
-37.5	.14	.06	.35	.13	1.53	.35	4.09	.62	14.01	1.94	19872	1.61	.14
-32.5	.43	.11	.37	.14	.34	.17	.80	.28	2.33	.78	18576	.54	.08
-27.5	.03	.03	.22	.11	.09	.09	0.00	0.00	.54	.38	17855	.11	.04
-22.5	0.00	0.00	0.00	0.00	0.00	0.00	0.00	0.00	0.00	0.00	18252	0.00	0.00
-17.5	0.00	0.00	0.00	0.00	0.00	0.00	0.00	0.00	0.00	0.00	8820	0.00	0.00

OMNIDIRECTIONAL FLUX SUMMARY VS LATITUDE FOR LONGITUDE= 52.5
LAT + 5 ENERGIES WITH RMS ERROR + NO OF OBS + LINE TOTALS

-52.5	0.00	0.00	0.00	0.00	0.00	0.00	0.00	0.00	0.00	0.00	9984	0.00	0.00
-47.5	.03	.03	0.00	0.00	.07	.07	.51	.21	2.45	.74	21528	.21	.05
-42.5	.05	.04	.05	.05	.38	.17	.97	.29	9.17	1.45	20940	.68	.09
-37.5	.08	.05	.05	.05	.08	.08	.27	.16	.47	.34	20220	.12	.04
-32.5	0.00	0.00	0.00	0.00	.09	.09	0.00	0.00	.26	.26	18780	.03	.02
-27.5	0.00	0.00	0.00	0.00	0.00	0.00	.48	.24	.63	.44	15324	.09	.04
-22.5	0.00	0.00	0.00	0.00	0.00	0.00	0.00	0.00	0.00	0.00	4536	0.00	0.00

P72-1 PROCESSING BEGUN IN OMSDJ 16/07/73 15.14.32. FILE NO.

LONGITUDE SUMMARY

LONG + 5 ENERGIES + NO OF OBS + LINE TOTAL

222.5	0	1	3	0	0	[illegible]4572	4
227.5	0	0	0	0	0	41172	0
232.5	0	0	0	0	0	51984	0
237.5	1	0	0	0	0	57192	1
242.5	1	0	0	0	0	77616	1
247.5	0	0	0	0	0	72131	0
252.5	0	1	0	0	0	64248	1
257.5	3	0	0	0	0	65100	3
262.5	0	0	0	0	0	61236	0
267.5	5	4	3	1	3	90912	16
272.5	18	11	8	8	1	96660	46
277.5	90	29	32	23	11	92291	185
282.5	221	151	70	84	28	[illegible]6544	554
287.5	585	333	215	221	83	99815	1437
292.5	1262	761	486	443	178	135717	3150
297.5	3298	2011	1223	1262	468	178151	8262
302.5	6059	3781	2276	2439	1030	216921	15585
307.5	8267	5490	3456	4272	1948	241420	23463
312.5	8573	5540	3777	5103	2579	244248	25572
317.5	7774	5273	3723	5673	3155	213922	25598
322.5	5322	3900	3100	5889	4014	171956	22225
327.5	3689	2642	2226	4941	3907	141663	17405
332.5	2514	1825	1655	3813	3087	119332	12894
337.5	2300	1618	1361	2969	2522	121799	10770
342.5	2655	1989	1729	3892	3409	102908	13674
347.5	1380	1280	1405	4878	5122	80591	14065
352.5	720	521	711	2259	2690	74285	7001
357.5	552	410	397	1086	1172	72786	3617
2.5	284	327	465	1856	2502	50251	5434
7.5	209	231	326	1576	2345	53255	4687
12.5	270	237	250	905	1015	[illegible]2456	2677
17.5	335	376	400	1643	2436	122358	5190
22.5	364	444	676	2813	4193	153858	8490
27.5	404	466	638	2556	3706	187680	7770
32.5	241	273	335	1534	2169	177772	4552
37.5	160	190	275	975	1406	158928	3006
42.5	76	85	127	453	667	158340	1408
47.5	22	20	38	115	209	176164	404
52.5	6	2	8	24	56	111312	96
0.0	57660	40342	31424	55706	56111	4509551	249243

B22

P72-1 PROCESSING BEGUN IN OMSDJ 06/07/78 15.14.32. FILE NO. 1

PITCH ANGLE SUMMARY

PA + 5 ENERGIES + NO OF OBS + LINE TOTAL

89	6715	4632	3767	8557	7632	102288	31507
87	6565	4544	3550	8453	7499	102545	30921
85	6324	4474	3595	7375	6997	101951	29265
83	6094	4248	3451	7447	6618	102713	27858
81	5355	3820	3106	6495	5808	102090	24584
79	4966	3784	2792	5521	5017	102425	21680
77	4304	3015	2375	4779	4182	102556	18656
75	3615	2437	1955	3353	3420	102530	15380
73	2897	2043	1554	2959	2560	102406	12013
71	2479	1593	1207	2245	2002	102716	9526
69	1800	1243	908	1538	1479	102775	7068
67	1421	1005	634	1050	981	102657	5101
65	999	705	431	708	657	102985	3503
63	755	522	349	365	381	102944	2392
61	535	379	227	301	213	102903	1655
59	381	263	158	216	112	103343	1130
57	310	231	121	111	64	103213	837
55	237	172	98	102	50	103520	659
53	169	140	69	77	33	103743	488
51	176	122	80	74	32	103892	484
49	129	100	73	59	24	104242	385
47	126	71	54	46	25	104110	325
45	97	97	48	59	31	104419	332
43	83	80	40	52	22	105175	277
41	99	60	43	46	15	105461	263
39	78	62	31	42	17	106758	230
37	74	55	33	31	10	106730	203
35	68	50	36	27	23	107908	204
33	62	55	27	29	22	108668	196
31	54	45	27	29	16	110410	171
29	687	490	285	320	168	1389275	1950
0	57660	40342	31424	63706	56111	4509551	249243

P72-1 PROCESSING BEGUN IN OMSDJ 05/07/78 15.14.32. FILE NO. 1

LAT SUMMARY

LAT + 5 ENERGIES + NO OF OBS + LINE TOTAL

-67.5	2	1	3	9	54	158039	69
-62.5	18	15	45	242	493	164763	814
-57.5	70	137	265	1368	2211	211788	4051
-52.5	553	600	887	3875	5637	257565	11552
-47.5	1773	1710	2295	8037	9752	310207	23567
-42.5	4186	3647	4232	12521	13401	314921	37987
-37.5	7936	5951	5410	13458	11999	320832	44744
-32.5	11137	7807	5803	10207	6827	324698	41781
-27.5	11463	7598	4957	6450	2996	327067	33564
-22.5	9185	5869	3494	3514	1333	326563	23395
-17.5	6115	3800	2096	2182	749	334603	14942
-12.5	3389	1973	1229	1160	430	343575	8181
-7.5	1427	887	575	517	175	351807	3581
-2.5	337	203	140	144	50	358221	874
2.5	47	40	18	19	4	243396	128
7.5	2	4	4	3	0	171700	13
0.0	57660	40342	31424	63706	56111	4509551	249243

END OF FILE ON OMSDJ

OMSDJ PROCESSING TIME 79.884

PHG/R. C. Filz/3240

11 July 1978

1972-076B-01

Dr. J. I. Vette
NSSDC
NASA Goddard Space Flight Center
Greenbelt, MD

Dear Jim

As promised I am sending you a computer magnetic tape (Label Vette 3) which contains a complete set of raw data from the particle identifier instrument flown on Air Force flight 72-1. A data set description and sample program with output are also included.

The data have been cumulated in a $1^{\circ} \times 1^{\circ}$ latitude - longitude sort for the period October 2, 1972 through Feb 1973. Since the 72-1 satellite orbit was circular, lying between the limits 740-760 Km during this period one can assign an altitude of 750 Km with little error. The $1^{\circ} \times 1^{\circ}$ grid is sufficiently small to allow the calculation of the magnetic field parameters B and L for the central point and apply them to all of the data obtained within the grid boundaries.

PHG

For each $1^{\circ} \times 1^{\circ}$ grid the data are given for five energy intervals - (45.0 to 28.0) (28.0 to 18.2), (18.2 - 12.2), (12.2 - 7.0), and (7.0 to 5.0) MeV and 31 pitch angle intervals with the boundaries - 90, 88, 86, 84, 82, 80, 78, 76, 74, 72, 70, 68, 66, 64, 62, 60, 58, 56, 54, 52, 50, 48, 46, 44, 42, 40, 38, 36, 34, 32, 30 and 0°. These intervals were assigned using the IGRF 1965 model magnetic field for the date 1973.0. The azimuthal angle is unspecified but should be unimportant for the following reasons:

PH

1. The proton telescope axis is spinning in the satellite orbital plane (98.4° inclination).

2. The declination in the magnetic field does not vary too much within the South Atlantic anomaly.

3. The trapped proton gyroradii are less than ~ 50 Km and hence with the above conditions the guiding center altitude is about the same as the satellite altitude.

4. Any real variations should be averaged between the N → S and S → N passes.

PH, SUSC, PHG, Mr. Filz

The largest error in the pitch angle variation should come from errors in the model field. The narrow width of the pitch angle distributions (page B 23) suggest no problem with the mirror plane directional flux ($j_\perp$): however, all things considered, the assignment of a guiding center altitude of 750 ± 10 Km to the data is probably justified. The minimum guiding center altitude is then dependent on B and L but never greater than 750 Km.

If you have any problems reading the tape or analyzing the data let me know. For format details, etc. call Ernie Holeman directly at (617)-862-0239. I will be away this summer from 17 July to 28 August so Ernie would be the best one to talk to during that period.

Sincerely

ROBERT C. FILZ
Magnetospheric Dynamics Branch
Space Physics Division

72-076B-01A

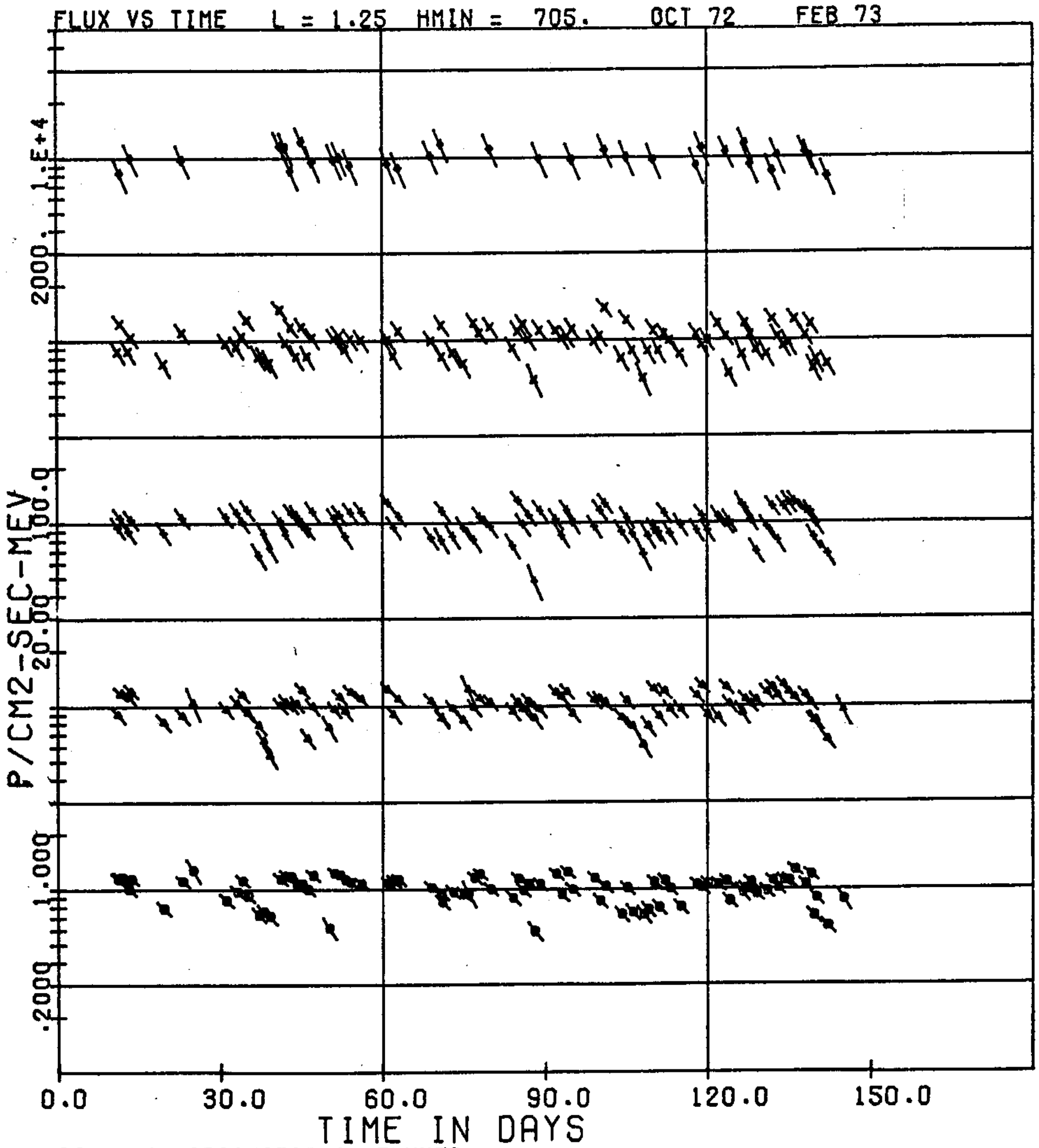

S72-1 OMNIDIRECTIONAL FLUXES.
CURVE AVGS 37.95. 41.01. 38.61. 43.25. 45.15
⊙ 36 MEV △ 23 MEV + 15 MEV × 9 MEV ◇ 6 MEV

RADSAT

DUMP OF TAPE ~~X416~~ D-31971, C-20126

INPUT TAPE X416 ON MS4

DATA INPUT H9 NF 5 FL 1 2 2 SR 5 1 2 SR 5 LAST 2

FILE 1 RECORD 1 LENGTH 3615BYTES

(0)	00000000	00000200	00000000	00000F00	00000000	0CC05000	00000000	00060000	00000000	0060C000
(40)	00000000	05000000	00000000	70000000	00000005	0CCC0000	00000080	00000000	00000500	0000C000
(80)	00006000	00000000	00070000	00000000	00400000	0CCC0000	07000000	00000000	70000000	00000004
(120)	00000000	00000070	00000000	00000600	00000000	0CCC5000	00000000	00070000	00000000	00500000
(160)	00000000	04000000	00000000	70000000	00000005	0CCC0000	00000060	00000000	00000600	00000000
(200)	00005000	00000000	00060000	00000000	00600000	0CCC0000	04000000	00000000	80000000	00000005
(240)	00000000	000004E0	00000000	00003F00	00000000	0CCCD000	00000000	000F0000	00000000	00E00000
(280)	00000000	0F000000	00000000	F0000000	0000000E	0CCC0000	000000D0	00000000	00000E00	00000000
(320)	0000D000	00000000	000D0000	00000000	00D00000	0CC00000	0D000000	00000000	E0000000	0000000C
(360)	00000000	000000F0	00000000	00000F00	00000000	0CCCE000	00000000	000E0000	00000000	00D00000
(400)	00000000	0F000000	00000000	E0000000	0000000E	0CCC0000	00000100	00000000	00001000	00000000
(440)	0000E000	00000000	000F0000	00000000	01000000	0CC00000	0F000000	00000001	10000000	0000000E
(480)	00000000	00000D00	00000000	00004000	00000000	0CC10000	00000000	000F0000	00000000	00D00000
(520)	00000000	10000000	00000000	D0000000	0000000E	0CCC0000	00000100	00000000	00001100	00000000
(560)	0000E000	00000000	00100000	00000000	00F00000	0CC00000	0F000000	00000001	00000000	0000C011
(600)	00000000	000000F0	00000000	00000F00	00000000	0CC11000	00000000	000E0000	00000000	01000000
(640)	00000000	12000000	00000000	F0000000	0000000F	0CCC0000	000000F0	00000000	00000E00	00000000
(680)	00010000	00000000	00110000	00000000	00F00000	0CCC0000	12000000	00000000	F0000000	00000010
(720)	00000000	00000DC0	00000000	00004100	00000000	0CC12000	00000000	00130000	00000000	01300000
(760)	00000000	13000000	00000001	40000000	00000014	0CCC0000	00000120	00000000	00001500	00000000
(800)	00013000	00000000	00130000	00000000	01400000	0CC00000	12000000	00000001	60000000	00000011
(840)	00000000	00000150	00000000	00001400	00000000	0CC14000	00000000	00110000	00000000	01400000
(880)	00000000	12000000	00000001	00000000	00000016	0CCC0000	00000130	00000000	00001400	00000000
(920)	00014000	00000000	00120000	00000000	01200000	0CC00000	14000000	00000001	50000000	00000014
(960)	00000000	00001050	00000000	00004200	00000000	0CC11000	00000000	00120000	00000000	01200000
(1000)	00000000	12000000	00000001	20000000	00000011	0CC00000	00000130	00000000	00001000	00000000
(1040)	00011000	00000000	00130000	00000000	01200000	0CCC0000	12000000	00000001	10000000	00000013
(1080)	00000000	00000110	00000000	00001200	00000000	0CC13000	00000000	00120000	00000000	01300000
(1120)	00000000	11000000	00000001	40000000	00000011	0CCC0000	00000110	00000000	00001400	00000000
(1160)	00012000	00000000	00130000	00000000	01500000	0CC00000	12000000	00000001	20000000	00000015
(1200)	00000000	00001020	00000000	00004300	00000000	0CCCA000	00000000	000A0000	00000000	00A00000
(1240)	00000000	08000000	00000000	90000000	00000009	0CCC0000	00000090	00000000	00000800	00000000
(1280)	0000A000	00000000	00080000	00000000	00800000	0CC00000	09000000	00000000	70000000	0000000C
(1320)	00000000	00000080	00000000	00000800	00000000	0CCCB000	00000000	00090000	00000000	00900000
(1360)	00000000	0A000000	00000000	A0000000	0000000B	0CC00000	000000B0	00000000	00000900	00000000
(1400)	0000A000	00000000	000A0000	00000000	00900000	0CCC0000	0B000000	00000000	90000000	0CC0000A
(1440)	00000000	00000930	00000000	00004400	00000000	0CCCD000	00000000	00100000	00000000	00B00000
(1480)	00000000	0F000000	00000001	00000000	0000000B	0CCC0000	000000D0	00000000	00001300	00000000
(1520)	0000A000	00000000	000D0000	00000000	01000000	0CC00000	0C000000	00000000	F0000000	0000000E
(1560)	00000000	000000B0	00000000	00000F00	00000000	0CCCF000	00000000	000A0000	00000000	00E00000
(1600)	00000000	12000000	00000000	A0000000	0000000F	0CCC0000	000000F0	00000000	00000C00	00000000
(1640)	00013000	00000000	000D0000	00000000	00C00000	0CCC0000	12000000	00000000	D0000000	0000000E
(1680)	00000000	00000C20	00000000	00004500	00000000	0CC10000	00000000	000C0000	00000000	00F00000
(1720)	00000000	0F000000	00000000	E0000000	0000000F	0CC00000	00000110	00000000	00000D00	00000000
(1760)	00012000	00000000	000E0000	00000000	01000000	0CCC0000	0F000000	00000001	00000000	0000000E
(1800)	00000000	00000120	00000000	00001000	00000000	0CCCF000	00000000	00130000	00000000	00E00000
(1840)	00000000	0F000000	00000001	30000000	0000000D	0CCC0000	00000110	00000000	00001200	00000000
(1880)	0000C000	00000000	00140000	00000000	01300000	0CC00000	0B000000	00000001	50000000	00000012
(1920)	00000000	00000D10	00000000	00004600	00000000	0CCCF000	00000000	00120000	00000000	01000000
(1960)	00000000	0F000000	00000001	10000000	0000000F	0CC00000	00000110	00000000	00001000	00000000
(2000)	0000E000	00000000	00100000	00000000	00F00000	0CC00000	0E000000	00000000	F0000000	00000013
(2040)	00000000	000000D0	00000000	00000E00	00000000	0CC11000	00000000	000F0000	00000000	01000000
(2080)	00000000	12000000	00000000	B0000000	00000015	0CCC0000	000000F0	00000000	00000D00	00000000
(2120)	00013000	00000000	000C0000	00000000	00F00000	0CCC0000	15000000	00000000	D0000000	0000000E
(2160)	00000000	00000CB0	00000000	00004700	00000000	0CC14000	00000000	00140000	00000000	01100000
(2200)	00000000	15000000	00000001	30000000	00000012	0CCC0000	00000140	00000000	00001400	00000000
(2240)	00012000	00000000	00160000	00000000	01100000	0CCC0000	14000000	00000001	40000000	00000013
(2280)	00000000	00000120	00000000	00001300	00000000	0CC16000	00000000	00100000	00000000	01500000

(2520)	B6DB6DB6	DB6DB6DB	6DB6DB6D	B6DB6DB6	DB6DB6DB	6DB6DB6D	B6DB6DB6	DB6DB6DB	6DB6DB6D	B6DB6DB6
(2560)	DB6DB6DB	6DB6DB6D	B6DB6DB6	DB6DB6DB	6DB6DB6D	B6DB6DB6	DB6DB6DB	6DB6DB6D	B6DB6DB6	DB6DB6DB
(2600)	6DB6DB6D	B6DB6DB6	DB6DB6DB	6DB6DB6D	B6DB6DB6	DB6DB6DB	6DB6DB6D	B6DB6DB6	DB6DB6DB	6DB6DB6D
(2640)	B6DB6DB6	DB6DB6DB	6DB6DB6D	B6DB6DB6	DB6DB6DB	6DB6DB6D	B6DB6DB6	DB6DB6DB	6DB6DB6D	B6DB6DB6
(2680)	DB6DB6DB	6DB6DB6D	B6DB6DB6	DB6DB6DB	6DB6DB6D	B6DB6DB6	DB6DB6DB	6DB6DB6D	B6DB6DB6	DB6DB6DB
(2720)	6DB6DB6D	B6DB6DB6	DB6DB6DB	6DB6DB6D	B6DB6DB6	DB6DB6DB	6DB6DB6D	B6DB6DB6	DB6DB6DB	6DB6DB6D
(2760)	B6DB6DB6	DB6DB6DB	6DB6DB6D	B6DB6DB6	DB6DB6DB	6DB6DB6D	B6DB6DB6	DB6DB6DB	6DB6DB6D	B6DB6DB6
(2800)	DB6DB6DB	6DB6DB6D	B6DB6DB6	DB6DB6DB	6DB6DB6D	B6DB6DB6	DB6DB6DB	6DB6DB6D	B6DB6DB6	DB6DB6DB
(2840)	6DB6DB6D	B6DB6DB6	DB6DB6DB	6DB6DB6D	B6DB6DB6	DE6DB6DB	6DB6DB6D	B6DB6DB6	DB6DB6DB	6DB6DB6D
(2880)	B6DB6DB6	DB6DB6DB	6DB6DB6D	B6DB6DB6	DB6DB6DB	6DE6DB6D	B6DB6DB6	DB6DB6DB	6DB6DB6D	B6DB6DB6
(2920)	DB6DB6DB	6DB6DB6D	B6DB6DB6	DB6DB6DB	6DB6DB6D	B6DB6DB6	DB6DB6DB	6DB6DB6D	B6DB6DB6	DB6DB6DB
(2960)	6DB6DB6D	B6DB6DB6	DB6DB6DB	6DB6DB6D	B6DB6DB6	DE6DB6DB	6DB6DB6D	B6DB6DB6	DB6DB6DB	6DB6DB6D
(3000)	B6DB6DB6	DB6DB6DB	6DB6DB6D	B6DB6DB6	DB6DB6DB	6DE6DB6D	B6DB6DB6	DB6DB6DB	6DB6DB6D	B6DB6DB6
(3040)	DB6DB6DB	6DB6DB6D	B6DB6DB6	DB6DB6DB	6DB6DB6D	B6DB6DB6	DB6DB6DB	6DB6DB6D	B6DB6DB6	DB6DB6DB
(3080)	6DB6DB6D	B6DB6DB6	DB6DB6DB	6DB6DB6D	B6DB6DB6	DB6DB6DB	6DB6DB6D	B6DB6DB6	DB6DB6DB	6DB6DB6D
(3120)	B6DB6DB6	DB6DB6DB	6DB6DB6D	B6DB6DB6	DB6DB6DB	6DE6DB6D	B6DB6DB6	DB6DB6DB	6DB6DB6D	B6DB6DB6
(3160)	DB6DB6DB	6DB6DB6D	B6DB6DB6	DB6DB6DB	6DB6DB6D	B6DB6DB6	DB6DB6DB	6DB6DB6D	B6DB6DB6	DB6DB6DB
(3200)	6DB6DB6D	B6DB6DB6	DB6DB6DB	6DB6DB6D	B6DB6DB6	DB6DB6DB	6DB6DB6D	B6DB6DB6	DB6DB6DB	6DB6DB6D
(3240)	B6DB6DB6	DB6DB6DB	6DB6DB6D	B6DB6DB6	DB6DB6DB	6DE6DB6D	B6DB6DB6	DB6DB6DB	6DB6DB6D	B6DB6DB6
(3280)	DB6DB6DB	6DB6DB6D	B6DB6DB6	DB6DB6DB	6DB6DB6D	B6DB6DB6	DB6DB6DB	6DB6DB6D	B6DB6DB6	DB6DB6DB
(3320)	6DB6DB6D	B6DB6DB6	DB6DB6DB	6DB6DB6D	B6DB6DB6	DE6DB6DB	6DB6DB6D	B6DB6DB6	DB6DB6DB	6DB6DB6D
(3360)	B6DB6DB6	DB6DB6DB	6DB6DB6D	B6DB6DB6	DB6DB6DB	6DB6DB6D	B6DB6DB6	DB6DB6DB	6DB6DB6D	B6DB6DB6
(3400)	DB6DB6DB	6DB6DB6D	B6DB6DB6	DB6DB6DB	6DB6DB6D	B6DB6DB6	DB6DB6DB	6DB6DB6D	B6DB6DB6	DB6DB6DB
(3440)	6DB6DB6D	B6DB6DB6	DB6DB6DB	6DB6DB6D	B6DB6DB6	DB6DB6DB	6DB6DB6D	B6DB6DB6	DB6DB6DB	6DB6DB6D
(3480)	B6DB6DB6	DB6DB6DB	6DB6DB6D	B6DB6DB6	DB6DB6DB	6DE6DB6D	B6DB6DB6	DB6DB6DB	6DB6DB6D	B6DB6DB6
(3520)	DB6DB6DB	6DB6DB6D	B6DB6DB6	DB6DB6DB	6DB6DB6D	B6DB6DB6	DB6DB6DB	6DB6DB6D	B6DB6DB6	DB6DB6DB
(3560)	6DB6DB6D	B6DB6DB6	DB6DB6DB	6DB6DB6D	B6DB6DB6	DB6DB6DB	6DB6DB6D	B6DB6DB6	DB6DB6DB	6DB6DB6D
(3600)	B6DB6DB6	DB6DB6DB	6DB6DB6D	B6DB6D						

FILE	INPUT RECS.	DATA RECORDS INPUT	MAX. SIZE	READ ERROR SUMMARY PERM	ZERO B	SHORT	UNDEF.	INPUT RETRIES #RECS.	TOTAL#
5	671	673	3615	0	2	0	0	2	2

EOJ DUMP STOPPED AFTER FILE 5 # OF PERMANENT READ ERRORS 0

START TIME 09/13/78 20:15:42 STOP TIME 09/13/78 20:17:52

$$